frontiers in Marine Science

ORIGINAL RESEARCH
published: 14 June 2019
doi: 10.3389/fmars.2019.00332

High Lability Fe Particles Sourced From Glacial Erosion Can Meet Previously Unaccounted Biological Demand: Heard Island, Southern Ocean

Pier van der Merwe[1], Kathrin Wuttig[1], Thomas Holmes[1,2], Thomas W. Trull[1,3], Zanna Chase[2], Ashley T. Townsend[4], Karsten Goemann[4] and Andrew R. Bowie[1,2]*

[1] Antarctic Climate and Ecosystems Cooperative Research Centre, University of Tasmania, Hobart, TAS, Australia, [2] Institute for Marine and Antarctic Studies, College of Sciences and Engineering, University of Tasmania, Hobart, TAS, Australia, [3] Commonwealth Scientific and Industrial Research Organisation, Hobart, TAS, Australia, [4] Central Science Laboratory, University of Tasmania, Hobart, TAS, Australia

OPEN ACCESS

Edited by:
Maeve Carroll Lohan, University of Southampton, United Kingdom

Reviewed by:
Jon Hawkings, Florida State University, United States
Mark James Hopwood, GEOMAR Helmholtz Centre for Ocean Research Kiel, Germany

***Correspondence:**
Pier van der Merwe
pier.vandermerwe@utas.edu.au

Specialty section:
This article was submitted to Marine Biogeochemistry, a section of the journal Frontiers in Marine Science

Received: *14 February 2019*
Accepted: *29 May 2019*
Published: *14 June 2019*

Citation:
van der Merwe P, Wuttig K, Holmes T, Trull TW, Chase Z, Townsend AT, Goemann K and Bowie AR (2019) High Lability Fe Particles Sourced From Glacial Erosion Can Meet Previously Unaccounted Biological Demand: Heard Island, Southern Ocean. Front. Mar. Sci. 6:332. doi: 10.3389/fmars.2019.00332

Iron (Fe) is an essential micronutrient that controls phytoplankton growth in the Southern Ocean. Dissolved Fe (<0.4 μm) has been extensively studied due to its relatively high bioavailability. However, particulate Fe (>0.4 μm) is far more abundant and may also become bioavailable through biogeochemical processing. To assess natural Fe fertilisation from the particulate fraction, we surveyed suspended particles in the water column at 11 stations in the vicinity of Heard and McDonald Islands (HIMI), in the Indian sector of the Southern Ocean and compared these to downstream plateau and reference stations. We quantified the labile (potentially bioavailable) fraction using a chemical leach. Suspended particles sourced from glacial erosion and fluvial outflow, including nanoparticulate Fe oxides near Heard Island, contained a significantly higher fraction of labile Fe (18 ± 2.8% of total Fe, or 115 ± 34 nM, n = 9) than all other coastal areas surveyed. In contrast, waters around McDonald Island, proximal to diffuse gasohydrothermal sites, contained poorly labile, highly refractory titanium and Fe bearing minerals such as ilmenite. We conclude that glacial erosion of Heard Island in combination with a unique elemental signature of the source rock, is an important mechanism of Fe supply to downstream waters. Our calculations show that the labile Fe supplied from primarily glacial erosion on Heard Island is sufficient to satisfy previously unmet estimates of phytoplankton demand for the region, and therefore critical to the area's productivity. As we move into a world facing major ecosystem shifts under a changing climate, it is important to understand those ecosystem services that may change into the future. At the current rate of glacier retreat, this ecosystem service of glacial erosion and Fe supply to coastal waters will cease with the eventual loss of glacial cover with direct impacts for this historically highly productive region.

Keywords: particulate trace metals, McDonald Island, suspended particles, chemical leach, hydrothermal, iron, labile particulate Fe, GEOTRACES

INTRODUCTION

The Southern Ocean maintains relatively little phytoplankton growth, despite a wealth of macronutrients (phosphate, nitrate + nitrite), due to a lack of micronutrients, principally the trace element iron (Fe) (de Baar et al., 2005; Boyd and Ellwood, 2010). Iron is supplied to the ocean through various forms of rock weathering and its physical and chemical form dictate whether phytoplankton and bacteria can utilise and then recycle it (Boyd et al., 2017). The Southern Ocean's anaemia is not ubiquitous. In fact, oases of abundant life exist in proximity to retreating sea ice (van der Merwe et al., 2009; Lannuzel et al., 2010, 2016), complex and shallow bathymetry (Mongin et al., 2008; Sherrell et al., 2018), in polynyas (Arrigo et al., 2015), at glacier fronts (Herraiz-Borreguero et al., 2016), and in the wake of Islands (Blain et al., 2007; Planquette et al., 2011). Each spring and into summer, a large phytoplankton bloom extends from the Kerguelen Plateau thousands of kilometres into the Southern Ocean (Schallenberg et al., 2018). Previous work has shown that weathering of Kerguelen Island, ∼500 km to the north (and north of the Polar Front), and the shallow plateaus surrounding it, supply the micronutrient Fe, temporarily alleviating Fe limitation and allowing the development of this bloom (Blain et al., 2007; Queroue et al., 2015; van der Merwe et al., 2015). However, the processes that supply Fe into waters surrounding Heard and McDonald Islands (HIMI), south of the Polar front, situated in significantly colder waters, are not well understood in terms of their magnitude and lability of the Fe supplied.

On the central Kerguelen Plateau, Heard and McDonald Islands, both part of the Australian Antarctic Territory, are close in distance (**Figure 1**), but unique in terms of their geology and glaciology. Heard Island is an active volcanic island, flanked by 12 glaciers. The intense mechanical rock weathering combined with subglacial aqueous biogeochemical weathering that occurs under glaciers produces fine rock particles known as glacial flour which can be high in Fe(II) and Fe(III) (Hawkings et al., 2014; Hopwood et al., 2014; Raiswell et al., 2018). Some of the glaciers on Heard Island terminate directly into the ocean, providing a direct transport pathway for particulate and dissolved Fe laden meltwater to fertilise adjacent seawater as has been observed in Alaska (Schroth et al., 2014). However, previous studies have cast some doubt on the effectiveness of Fe fertilisation from this source, suggesting instead that the majority of dissolved Fe is lost to depth due to flocculation almost immediately upon entering seawater (Zhang et al., 2015; Hopwood et al., 2015, 2016). Conversely and highlighting the complexity of this process, flocculated meltwater may actually extend horizontal transport away from a source, depending on the size, shape, and densities of the flocs produced (Markussen et al., 2016).

In contrast, McDonald Island has no glaciers at all, and is also volcanically active. Its smouldering mountain peaks are the result of a large eruption in the 1980s that saw the island double in size (Stephenson et al., 2005). In general, volcanoes can supply highly labile, Fe bearing ash to large areas of the ocean (Browning et al., 2015). Likewise, undersea hydrothermal vents, through fluid-rock chemical weathering at high temperature and low pH, can efficiently dissolve trace metals from bedrock, which upon entering oxygenated seawater, rapidly precipitate to form fine hydroxide or sulphide particles (Mottl and McConachy, 1990; Gartman et al., 2014). Furthermore, studies have shown that a proportion of these particles (unreactive Fe nanoparticles or colloids) as well as the dissolved trace metals (stabilised via organic complexation or by incorporation into inorganic or organic colloids) can be transported over long distances within the ocean (Lam et al., 2012; Fitzsimmons et al., 2014; Resing et al., 2015). However, many hydrothermal vents occur in deep water and while modelling studies predict a significant contribution to the surface dissolved Fe inventory (Tagliabue et al., 2010) the transport pathway to shallow, sunlit zones remains unclear (Holmes et al., 2017). The fascinating combination of glaciated and ice-free volcanic islands near each other provides an ideal test site to observe these unique forms of trace metal supply into the surrounding Fe-limited Southern Ocean.

Heard Island was actively erupting during the present campaign and lava flows were clearly visible running down the upper flanks of Mawson Peak and over the glaciers, only to disappear into the ice at some stage down slope (**Figure 2B**). McDonald Island was also displaying subaerial volcanic activity with steam rising from fumaroles on its flanking slopes. While the islands are close in distance, (43 km) Heard Island (368 km^2) has two orders of magnitude more surface area than McDonald Island (3 km^2). Furthermore, previous geochemical studies have noted the stark contrast between the phonolitic lavas on McDonald and the basanite-alkali basalt-trachyte series of Heard Island (Barling et al., 1994; Quilty and Wheller, 2000). Phonolites are uncommon extrusive igneous rocks with an intermediate chemical composition with undersaturated silica (SiO_2) and very high alkalies ($Na_2O + K_2O$), while basalts and trachybasalts are much more common extrusive igneous rocks (Quilty and Wheller, 2000). This interesting juxtaposition should result in unique sources of fertilising nutrients into the near-shore surrounding waters, however, the effect on distant, downstream waters is more uncertain.

Here, we investigate whether the unique processes of hydrothermal and glacial erosion dictate trace metal supply and lability into the downstream, highly productive waters. Specifically, is glacial erosion and sub-glacial meltwater outflow the main fertiliser of the large downstream phytoplankton bloom? In combination, what impact does the elemental composition of the source rock have on the resultant chemical lability of particles supplied? Finally, can the chemically labile pFe supplied from HIMI meet the previously unaccounted Fe demand over the plateau, downstream of the islands, where a large phytoplankton bloom develops seasonally? To achieve this, a comprehensive survey of the water column, suspended particles and underlying sediments was conducted near HIMI in January and February 2016 on board the RV Investigator. We use a chemical leach, reported by Berger et al. (2008) and recommended by Rauschenberg and Twining (2015) to differentiate the chemically refractory trace metal component of marine suspended particles from the chemically labile fraction. This gives some insight into the amount of trace metals supplied from these varying sources, and is one of the

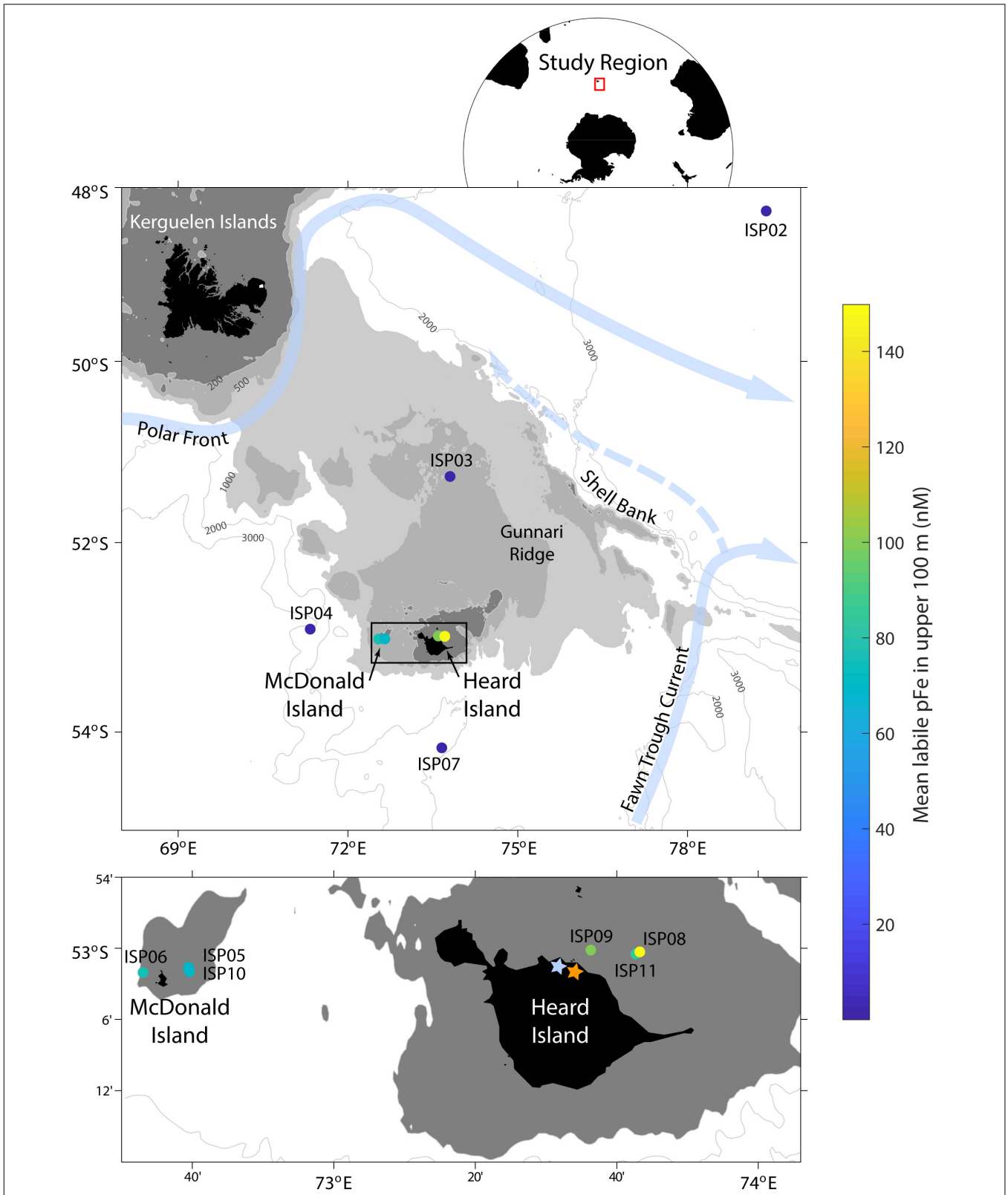

FIGURE 1 | Map of the study region during the Heard Earth-Ocean-Biosphere Interactions (HEOBI) cruise in January and February 2016. The mean concentration of labile particulate Fe (pFe_{lab}) in the upper 100 m at each station is indicated with a colour scale and main surface currents in light blue. Downes (blue star) and Ealey (orange star) marine terminating glaciers are also indicated on Heard Island. The low-Fe, reference stations were ISP2 and 7, the moderate-Fe plateau stations were ISP3 and 4, while our high-Fe near-shore stations were ISP5, 6, and 10 (McDonald Island) and ISP8, 9, and 11 (Heard Island).

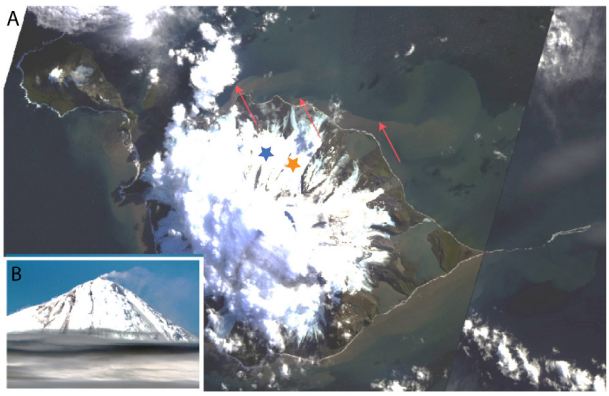

FIGURE 2 | Landsat 8 satellite image of Heard Island **(A)** with image of Mawson Peak, Heard Island, taken during the HEOBI voyage inset **(B)**. Sharp delineation can be seen between the outflowing, sediment laden, fluvial/subglacial meltwater on the north–east side of the island and the surrounding ocean. To the north of the island, outflow can be seen originating at the beginning of each major glacier terminus. Due to the east–north–east flowing surface currents, sediments are concentrated against the coastline on the south–west of the island, making outflow less obvious. Downes (blue star) and Ealey (orange star) marine terminating glaciers are shown. Red arrows indicate delineation between outflowing glacial water and seawater. Source satellite image: Google Earth (earth.google.com/web/), inset picture credit Pete Harmsen (Marine National Facility).

factors effecting the availability of particulate trace metals for phytoplankton uptake.

MATERIALS AND METHODS

Suspended Particles

All samples were collected during the GEOTRACES Process Study (GIpr05) as part of the Heard Earth-Ocean-Biosphere Interactions (HEOBI) voyage in January and February 2016 on board the RV Investigator. Sample handling, collection, and processing was performed in accordance with recommended GEOTRACES protocols[1], with specific methodologies used in our laboratory outlined in Bowie et al. (2010). Sampling locations were chosen to provide contrast between low Fe reference stations, moderate Fe plateau stations and high Fe near shore sites at both Heard and McDonald Islands (**Figure 1**). Suspended particles were collected using up to eight, McLane high volume, *in situ* pumps (WTS-LV) (here on referred to as ISPs) fitted with dual filter holders, featuring high efficiency baffles to dramatically reduce sample wash off upon sampler retrieval (in comparison to previous generation filter holder designs). Suspended particles for trace metal analysis were collected using paired, acid washed, 142 mm, 0.8 μm Supor filters to obtain a 0.4 μm effective pore size (Bishop et al., 2012). ISPs were deployed on 12 mm Dyneema at varying depths throughout the water column and pumping duration was generally 2 h, resulting in mean pumped volume of 170 L for Supor filters. Depths were chosen after viewing conductivity, temperature and depth (CTD) profiles to allow sampling within areas of interest. Mixed layer depths (MLD) were calculated with the gsw_mlp package of the Gibbs-SeaWater (GSW) Oceanographic Toolbox (McDougall and Barker, 2011) using continuously measured CTD profile data. This package calculates the MLD based on a threshold method, defined as the depth where a change in density of 0.03 kg m^{-3} or change in temperature of 0.2°C from a surface reference value is reached, as described in de Boyer Montégut et al. (2004). Temperature and salinity data were taken from Sea-Bird Electronics SBE3T and SBE4C sensors, respectively, which were mounted on the primary CTD rosette. Chlorophyll fluorescence was derived from a WETLABS FLBBRTD dual channel fluorometer also installed on the standard CTD. Nutrient samples were collected using the standard CTD rosette. Concentrations of NOx (NO_3^- and NO_2^-), NO_2^-, SiO_4^- and PO_4^{3-} were analysed on-board using a SEAL AA3 HR AutoAnalyzer (Rees et al., 2019). Throughout this work, Ultra-High Purity (UHP) water was supplied from a Milli-Q Advantage A10® and Q-Pod Element® (Merck Millipore).

Sequential Trace Metal Extraction of Suspended Particles

A chemical leach reported by Berger et al. (2008) and reviewed by Rauschenberg and Twining (2015) was used to separate the chemically refractory trace metal component of marine suspended particles from the chemically labile fraction. The review looked at the most common methods for determining bulk labile trace metals from marine suspended particulate samples. Based on elemental recoveries and practicality, the review recommended that the chemical leach used here (detailed below) was the most suitable (see Rauschenberg and Twining, 2015, for further details).

In situ pump filters (142 mm, Pall Supor PES) were subsampled using a custom-made Ti, 47 mm circular punch and polyethylene hammer above a 5 mm thick Teflon tile. Filters were processed inside an ISO 5 laminar flow hood, within a containerised clean room immediately after pump recovery. The filter subsamples were then placed into acid-washed petri dishes and frozen at −20°C until analysis.

At the home laboratory, the subsampled ISP filters (47 mm) were folded into quarters so that all particulate material was facing inward and then placed into acid-washed, 15 ml polypropylene centrifuge tubes (Falcon™) to contain all loose particulate material within the filter. One millilitre of a 25% (v:v) acetic acid (Seastar Chemicals, Baseline grade) and 0.02 M Hydroxylamine Hydrochloride solution was added directly to each filter within the centrifuge tubes. The filters were then immediately transferred into an oven set at 90–95°C for 10 min. After 10 min, the oven was set to ramp down to 30°C over 2 h. After this time, the filters were removed with acid washed, plastic tweezers, leaving the leachate behind, and placed into 15 ml, perfluoroalkoxy alkane (PFA) digestion vials (Savillex).

The remaining leachate solution in each 15 ml tube was centrifuged at 12,000 RCF for 10 min. Subsequently, 500 μl of leachate supernatant was removed carefully without disturbing

[1]http://www.geotraces.org/

any particles that may have gathered at the bottom of the vial and placed into an acid washed 15 ml Teflon vial (Savillex). Any residue that remained in the leachate tubes was rinsed into the vials containing the filters with 1 ml of UHP water. One hundred microliters of concentrated HNO_3 was then added to the leachate vial and the whole solution was evaporated to dryness at 70°C for 4 h. The dried-down leachate was then redissolved in 2 ml of 2% HNO_3 with internal standard ready for SF-ICP-MS analysis. The analysed leachate is hereafter referred to as labile particulate trace metals, or for Fe, pFe_{lab}.

The vials containing the filters and undissolved leachate residue were now subjected to a total acid digestion as follows. A 4 M (after 1 ml UHP leachate rinse) mixed solution of HCl, HNO_3 and HF (all Seastar Chemicals, Baseline grade) acid was freshly prepared and 2 ml added to each vial to completely submerge the filter following a modified method of Bowie et al. (2010) and Ohnemus et al. (2014). Filter blanks, which were mounted onto the ISPs but not deployed into the ocean, were prepared in the same manner and followed the entire leach and analysis process and are reported in **Table 1**. Samples were then digested for 12 h at 95°C on a Teflon coated hotplate (SCP Science Digiprep). After this time, the filter was removed and rinsed with ultra-high purity water back into the digestion vial. The digestion vial was then evaporated to dryness at 70°C overnight. Once dry, 2 ml of 50% (v/v) HNO_3 (Seastar chemicals Baseline grade) acid was added and evaporated to dryness again. Finally, 10 ml of 2% HNO_3 with indium (In) internal standard included was added to each vial to redissolve the digest material ready for SF-ICP-MS analysis. This fraction hereafter referred to as the refractory particulate trace metals. Four random samples were run in duplicate through the full sequential digestion and compared in **Table 2**. Six random filter sub-samples were also analysed by a single total digestion and the results compared to the sum of the labile and refractory fractions for quality assurance and are presented in **Table 3**. There is currently no certified reference material (CRM) suitable for a sequential leach such as this, although efforts are underway by colleagues to rectify this. Here, we use the total digestion of CRM detailed below (see the section "Sediment") for quality assurance.

Sediment

Sediment samples were collected using either a Smith-McIntyre grab sampler or a dredge. The Smith-McIntyre grab is a commercially available sediment sampler which uses spring-activated buckets to collect a seafloor sediment sample over an area of 0.2 m^2. Upon retrieval, a small subsample of sediment was removed and placed into an acid-washed, 10 ml polypropylene tube (Sarstedt) and frozen at −20°C until analysis at the home laboratory. The sediment was ground and homogenised using a mortar and pestle then dried overnight at 60°C. Approximately 40 mg was weighed into 15 ml Teflon digestion vials. The sediment samples were then subjected to the same total digestion method as above (section "Sequential Trace Metal Extraction of Suspended Particles") with the only modification being that 4 ml of 4 M acid solution was added to the sediment samples due to their larger sample weight. Certified reference materials MESS-3 and BCR-414 were also processed through the above procedure and analysed in triplicate (**Table 4**). Elemental recoveries for Fe, Al, Mn, and Ti were within the analytical uncertainty of certified values or those values reported in the literature (where available). Acid blanks were prepared as above and analysed in triplicate to determine the limit of detection (3 × SD of the blank) (**Table 1**). The mean blank was subtracted from all measured sample concentrations. The sediments were not leached to determine their chemical lability.

TABLE 1 | Blanks and associated statistics for the SF-ICP-MS analysis in μg/L.

	Refractory				Labile				Totals, sediments, and CRMs			
μg/l	**Al**	**Ti**	**Mn**	**Fe**	**Al**	**Ti**	**Mn**	**Fe**	**Al**	**Ti**	**Mn**	**Fe**
Blank R1	20.0	3.7	0.2	12.2	4.1	0.1	0.1	2.7	1.4	4.7	0.1	3.4
Blank R2	3.1	1.7	0.1	4.3	5.1	0.2	0.1	2.9	2.0	1.8	0.1	4.9
Blank R3	5.0	1.7	0.1	6.4	7.6	0.1	0.1	2.6	2.3	1.4	0.1	4.3
Blank R4	18.9	2.5	0.1	5.9	7.7	0.1	0.1	2.3	1.1	0.3	0.0	1.2
Mean	11.7	2.4	0.1	7.2	6.1	0.1	0.1	2.6	1.7	2.0	0.1	3.5
RSD (%)	76	40	48	48	30	21	7.8	10	34	91	54	47
LOD	26.9	2.8	0.2	10.4	5.6	0.1	0.01	0.8	1.7	5.6	0.1	4.8

Blanks R1–R4 were blanks appropriate for each analysis (refractory, labile, and totals). For the refractory and labile analysis, the blanks consisted of filters that were loaded onto the ISP filter stages but not deployed in the ocean and then subjected to the full sequential trace metal extraction detailed in section "Sequential Trace Metal Extraction of Suspended Particles." For the total, sediments and CRMs, the blanks consisted of total digestion acids, dried down and resuspended as per the samples. It should be noted that the LOD is only applicable to the sample introduced to the ICP, and not applicable to the LOD for trace metals in seawater by this method as the in situ pumps concentrate between 2 and 48 L of seawater onto each 47 mm subsample. Generally, the lower the ambient concentration of trace metals, the higher the flow rate of the in situ pumps, resulting in higher concentration factors when ambient concentrations are lower. All samples below the LOD were excluded during data processing and were not presented in this work.

TABLE 2 | Duplicate subsamples from the *in situ* pump filters were subjected to the full sequential trace metal extraction and are shown to illustrate the full process error typical for the analysis.

	Station name	Pump #	Depth (m)	Al (nM)	Ti (nM)	Mn (nM)	Fe (nM)
Refractory	ISP05	1	105	1447	297	11.7	722
	ISP05	1	105	567	236	9.4	594
	ISP08	4	15	782	323	8.9	681
	ISP08	4	15	446	313	9.2	714
	ISP09	1	30	631	183	5.5	418
	ISP09	1	30	390	180	5.5	400
	ISP10	3	60	1354	236	13.4	668
	ISP10	3	60	1230	218	12.2	597
Labile	ISP05	1	105	404	0.6	1.4	84.1
	ISP05	1	105	359	0.4	1.3	78.9
	ISP08	4	15	123	0.8	2.4	156
	ISP08	4	15	135	0.8	2.7	175
	ISP09	1	30	97.8	1.2	1.4	91.1
	ISP09	1	30	113	1.4	1.7	111
	ISP10	3	60	1130	1.0	1.4	75.5
	ISP10	3	60	1230	1.0	1.6	83.1

Particulate trace metal concentrations in seawater are presented in nM.

TABLE 3 | Comparison between three independent measurements of six replicates of suspended particles collected during the HEOBI voyage.

% Recovery	Al	Ti	Mn	Fe
R1	40	119	102	99
R2	70	133	112	109
R3	70	155	134	118
R4	78	134	110	103
R5	88	162	111	113
R6	101	161	117	118
Mean	74	144	114	110
SD	21	18	11	8
RSD (%)	28	13	10	7

Subsamples of filters loaded with suspended particles were analysed by a total digestion and compared to the sum of labile and refractory trace metal fractions. Below we present the labile + refractory/total (×100) which represents the recovery of the total trace elements by the sequential digestion used during this work.

TABLE 4 | Results of the analysis of certified reference materials BCR_414 (freshwater plankton) for trace elements and MESS_3 marine sediment reference material for trace elements.

	Al	Ti	Mn	Fe
BCR_414_R1	2.78	0.03	0.29	1.85
BCR_414_R2	2.73	0.05	0.28	1.80
BCR_414_R3	2.63	0.02	0.27	1.75
Mean	2.72	0.04	0.28	1.80
SD	0.08	0.01	0.01	0.05
RSD (%)	3	38	4	3
Certified	n/a	n/a	0.299	1.85
Error	n/a	n/a	0.013	0.19
Recovery (%)	n/a	n/a	94	97
MESS_3_R1	85.6	4.3	[0.60]	42.7
MESS_3_R2	76.2	4.2	0.33	41.8
MESS_3_R3	83.5	4.4	0.34	42.8
Mean	81.8	4.3	0.34	42.4
SD	4.9	0.10	0.01	0.6
RSD (%)	6	2	2	1
Certified	85.9	4.4	0.324	43.4
Error	2.3	0.6	0.012	1.1
Recovery (%)	95	98	104	98

Mean, standard deviation (SD), and relative standard deviation (RSD) are shown for the triplicate analysis alongside the certified value and certified error. The percentage recovery between the mean of our analysis and the certified value is also presented. A single outlier for Mn is highlighted with square brackets and was not used for statistics as this data was likely an error on the ICP-MS as Mn is not a common contaminant.

Trace Metal Analysis: SF-ICP-MS

Samples were analysed for a full suite of 20 elements using a Thermo Fisher Scientific, Element 2, SF-ICP-MS. To maintain focus, here we consider only Fe, Al, Mn, and Ti. A low contamination front end was installed on the SF-ICP-MS prior to analysis and the system was acid washed thoroughly. Samples were introduced to the system as 2% HNO_3 solutions within a HEPA filtered air cabinet. The instrument was operated with guard electrode activated, increasing sensitivity 10- to 20-fold (Appelblad et al., 2000). All standards and samples contained 10 μg/l In as an internal standard and were prepared volumetrically via serial dilution. Instrument drift throughout each day of analysis was monitored using 5 μg/l mixed standard solutions, analysed periodically after approximately 10 samples. Following mixed standard calibration, multiple rinse solutions of 2% HNO_3 were analysed to confirm low level background levels of the SF-ICP-MS. Further instrument method details have been presented previously (Bowie et al., 2010).

Dissolved Fe

A complete analysis of the dissolved trace elements during this voyage including detailed methods can be found at Holmes et al. (2019). All protocols are based on standard GEOTRACES operating procedures (see text footnote 1). Briefly, dissolved trace elements were collected using a 12-bottle, trace-metal-clean rosette deployed on metal-free Dyneema and processed inside a containerised clean room. Samples were filtered at 0.2 μm, acidified to pH 1.8 (Baseline HCl, Seastar Chemicals) and stored at ambient clean-lab conditions until analysis. Samples were preconcentrated using a sea*FAST* S2 Pico, utilising Nobias PA1 resin and analysed on a Thermo Fisher Scientific, Element 2, SF-ICP-MS after intensive analytical quality control as previously published (Wuttig et al., 2019).

SEM Imaging

Filter subsamples (16 mm diameter) were attached to 12 mm or 25 mm diameter aluminium SEM mounts using double-sided sticky carbon tabs and coated with around 20 nm of carbon using a Ladd 40000 carbon evaporator. Scanning electron microscopy (SEM) and energy-dispersive X-ray spectrometry (EDS) were carried out on a Hitachi SU-70 field emission SEM fitted with an Oxford AZtec XMax80 EDS system at the Central Science Laboratory, University of Tasmania. Electron beam conditions were 15 kV accelerating voltage and around 3 nA probe current. Elemental compositions can be considered semiquantitative only due to the complex shape and small size of the particles investigated. EDS X-ray spectra frequently contain contributions from adjoining mineral grains and/or the filter substrate. The small particle size also prohibited mounting in epoxy and polishing to a flat surface. To overcome variability in individual particle analyses, approximately 50 particles of each type at each site were analysed and then the mean composition was entered into a mineral identification software (MinIdent-Win 4, Micronex, Canada) to determine mineralogy.

RESULTS

The results of particle leaches using the method of Berger et al. (2008) revealed the labile fraction of particles at each contrasting region within the study (**Figure 3**). Overall, most particulate trace metals collected near Heard and McDonald Islands were refractory, with a lithogenic origin. On average, particulate Fe, manganese (Mn), and titanium (Ti) were 88, 88 and 99% refractory, respectively, at McDonald Island. In contrast, at Heard Island, particulate Fe, Mn, and Ti were 78, 74, and 99% refractory, respectively. On average, the fraction of refractory Fe decreased

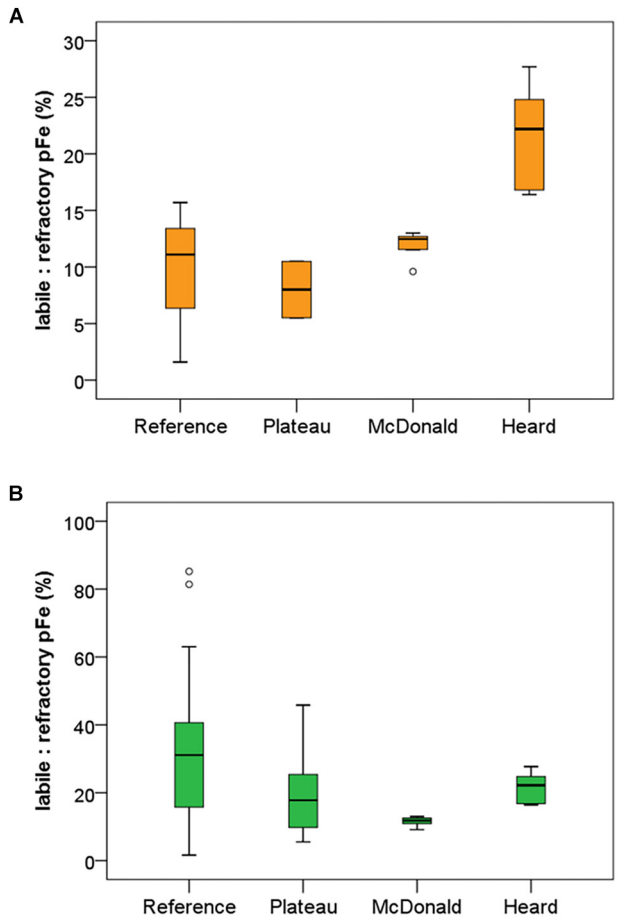

FIGURE 3 | Mean labile fraction of pFe (ratio of labile to refractory pFe) at each of the contrasting regions within the study. Labile fraction of pFe is shown within the mixed layer only **(A)** and within the full water column **(B)**. Standard boxplot median (centre black line), 25th and 75th percentiles (upper and lower box limits) and 95% confidence intervals (inner fences) are indicated. Outliers are shown as open circles and defined as less than 1.5 times the interquartile range. The number of independent data points for the reference, plateau, McDonald and Heard regions were 3, 2, 8, and 9 for panel a and 15, 13, 12, and 9 for panel **(A)**, respectively. Variability is generally lower near Heard and McDonald Islands due to the water column being well mixed in comparison to the reference and plateau stations.

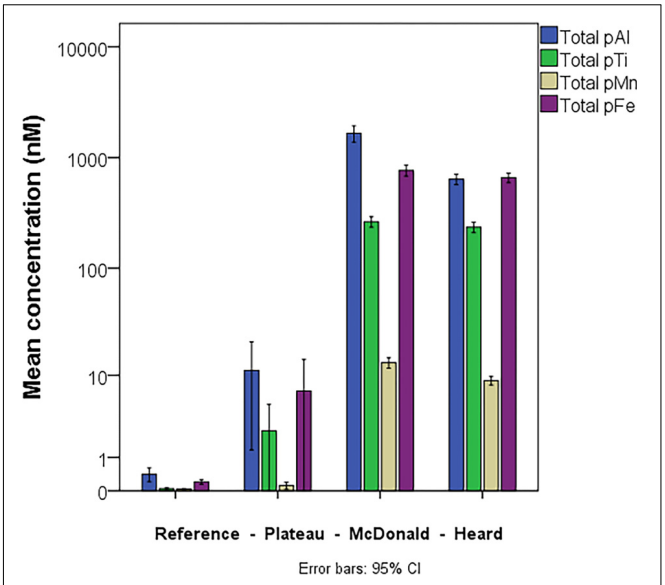

FIGURE 4 | Mean, full water column, total particulate (labile + refractory) Al, Ti, Mn, and Fe within the suspended particles at the four contrasting regions within the study. Error bars represent the 95% confidence interval. The number of independent data points for the reference, plateau, McDonald and Heard regions were 15, 13, 12, and 9, respectively.

with distance from the islands: 80 and 65% at the plateau and reference site, respectively, when considering the whole water column, and generally decreased with depth over the plateau and reference stations (**Figure 3B**). This trend with distance from the islands is driven by higher concentrations of labile trace metals at depth and is less evident or reversed if only considering the surface mixed layer (**Figure 3A**). While total particulate Fe, aluminium (Al), Mn, and Ti were all higher at the stations sampled around McDonald Island (**Figure 4**), the fraction of Fe that was labile was significantly higher at Heard Island compared to McDonald Island (one-way ANOVA, $p < 0.01$). In fact, when looking at the suspended particles within the mixed layer only across the four regions of interest (**Figure 3A**), Heard Island displayed a significantly higher mean labile fraction compared to all other sites, including the reference station (one-way ANOVA, Games-Howell *post hoc*, $p < 0.01$). Furthermore, in addition to the ratio of labile to refractory Fe being higher at Heard Island, the absolute concentration of labile particulate Fe (pFe_{lab}) was also significantly higher at Heard Island (115 ± 34 nM, $n = 9$) compared to McDonald Island (79 ± 20 nM, $n = 12$) (one-way ANOVA, Games-Howell *post hoc*, $p < 0.01$) (**Figure 5**). Although the reference station displayed the highest fraction of mean labile Fe across the full water column, the highly labile particles were found below the mixed layer at depths typically associated with dominant heterotroph recycling (Trull et al., 2008) (**Figure 3B**). The plateau station had mixed layer labile Fe fractions similar to the reference station mean, and higher concentrations below the mixed layer.

SEM analysis revealed that Ti and Fe bearing minerals such as ilmenite ($FeTiO_3$) were ubiquitous at the near shore sites (**Figure 6B**). Some micas and feldspar/alkali-feldspars ($KAlSi_3O_8$ – $NaAlSi_3O_8$ – $CaAl_2Si_2O_8$) were observed at both Heard and McDonald Island also, although with lower frequency. At Heard Island, specifically near direct glacier discharge at station 9, Fe oxides and/or hydroxides were observed. These cannot be distinguished further by SEM-EDS analysis as hydrogen (H) cannot be measured and the magnitude of the error of the measured Fe/O ratio is unknown for rough, small particles. Some Fe oxides and/or hydroxides were also observed at McDonald Island however, none were observed at the reference station. Fe-oxides or hydroxides from Heard and McDonald Islands were observed in the <1 μm size range, extending into the nanoparticle size range (<100 nm) (**Figure 6A**). Small particles of ilmenite were also observed in the nanoparticle size

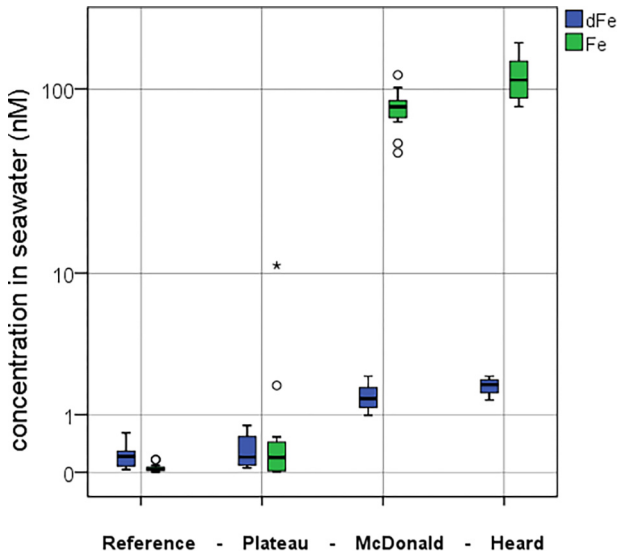

FIGURE 5 | Comparison between the mean dFe (blue) and mean pFe_{lab} (green) concentrations at the four contrasting regions during the study. Full water column means are presented in nM. Standard boxplot median (centre black line), 25th and 75th percentiles (upper and lower box limits) and 95% confidence intervals (inner fences) are indicated. Outliers are shown as circles (<1.5 × the interquartile range) and asterisk (>1.5 × the interquartile range). The number of independent data points for the reference, plateau, McDonald and Heard regions were 15, 13, 12, and 9 for pFe_{lab} and 16, 14, 12, and 9 for dFe, respectively.

range. At the reference site, only barite ($BaSO_4$) was observed in this analysis.

The mean concentration of pFe_{lab} was low at the reference station (0.05 ± 0.05 nM, $n = 15$) in comparison to mean dissolved Fe (dFe) (0.24 ± 0.17 nM, $n = 16$) (**Figure 5**), while over the plateau it was slightly higher (pFe_{lab} was 1.1 ± 3.0 nM, $n = 13$ and dFe was 0.31 ± 0.25 nM, $n = 14$). Conversely, near Heard Island mean pFe_{lab} was two orders of magnitude more enriched (115 ± 34 nM, $n = 9$) than the mean dFe concentration (1.8 ± 0.27 nM, $n = 9$). Likewise, at McDonald Island, pFe_{lab} was (79 ± 20 nM, $n = 12$) while mean dFe concentration was (1.5 ± 0.44 nM, $n = 12$). We observed a significant difference in pFe_{lab} between Heard and McDonald Islands as well as between the reference station and McDonald Island (one-way ANOVA, Games-Howell *post hoc*, log-transformed data, $p < 0.01$).

Salinity and temperature data from the ship's underway systems revealed that the surface waters adjacent to glacial outflow near Heard Island were fresher and somewhat warmer than the rest of the surface waters around Heard Island (**Figure 7**). In contrast, the surface waters around McDonald Island were more saline and colder than the surface waters near Heard Island or over the plateau. Vertical profiles of salinity and temperature near the islands reveals a well-mixed water column, particularly near Heard Island. Warmer and fresher water was present at Heard Island compared to McDonald Island from the surface to the seafloor (**Figure 8**). Combining dFe data from Holmes et al. (2019) with CTD data from the trace metal rosette, we observed a significant positive linear relationship between salinity and dFe as well as pFe_{lab} at the reference and plateau stations (**Table 5**). Salinity throughout the full water column correlates significantly with NO_X, nitrite (inv), silicate and phosphate at the reference and plateau stations, while at the shallow waters near McDonald Island, salinity correlates with NO_X, nitrite (inv), silicate and both fractions of particulate Fe. However, near Heard Island a significant inverse linear relationship was observed between salinity and dFe, phosphate and silicate at Heard Island, but not at any other site.

Some clear distinctions emerged when looking at the ratio of various trace metals within the suspended particles collected close to HIMI (**Figure 9**). We observed a significant increase in the ratio of refractory Fe:Al near the islands in comparison to the reference station (one-way ANOVA, $p < 0.01$) (**Figure 9**). The reference and plateau stations were not significantly different in either refractory or labile Fe:Al. The labile Fe:Al ratio was approximately four times higher at Heard compared to McDonald Island, which was primarily driven by very high labile Al concentrations at McDonald, but also significantly higher labile Fe observed at Heard Island (one-way ANOVA, $p < 0.01$).

Satellite images of Heard Island during summer reveal sharp delineation between outflowing, sediment laden water and the surrounding seawater (**Figure 2A**). The sharp delineation that originates at the western extent of Downes marine terminating glacier could suggest that the brown tainted water is flowing from a point source. This feature is less obvious on the south western side of Heard Island due to the dominant north east flowing surface currents that concentrate outflow and shallow coastal sediment resuspension against the coastline. Although the system is complex with tidal flows and resuspension of shallow coastal sediment likely occurring simultaneously, the prominent outflow on the north east of the island likely originates from Downes and Ealey marine terminating glaciers with station 9 directly in the path of the outflow. During our occupation, Heard Island's active volcano, Big Ben, erupted and sent lava flowing over the north-eastern flanks of the island, which subsequently melted through the ice creating channels down the glaciers (**Figure 2B**).

The concentration of total (refractory + labile) trace metals within the suspended particles at the contrasting stations was heavily skewed toward the near shore stations proximal to the islands while the reference station had persistently low absolute concentrations of suspended trace metals. HIMI stations were three orders of magnitude higher than the reference station in full water column mean total pFe, pAl and pTi concentration, and two orders of magnitude higher than the plateau station (**Figure 4**). Despite its smaller size and surface area, the samples collected near McDonald Island displayed significantly higher concentrations of pAl and pMn (one-way ANOVA, $p < 0.01$) than at Heard Island, while total particulate Fe and Ti were not significantly different. It should be noted that the stations sampled near McDonald Island were on average 2.8 km from the shore, while the Heard Island stations were 5.3 km on average. Due to the larger area of Heard Island (368 km^2) compared to McDonald Island (3 km^2), the integrated total supply of

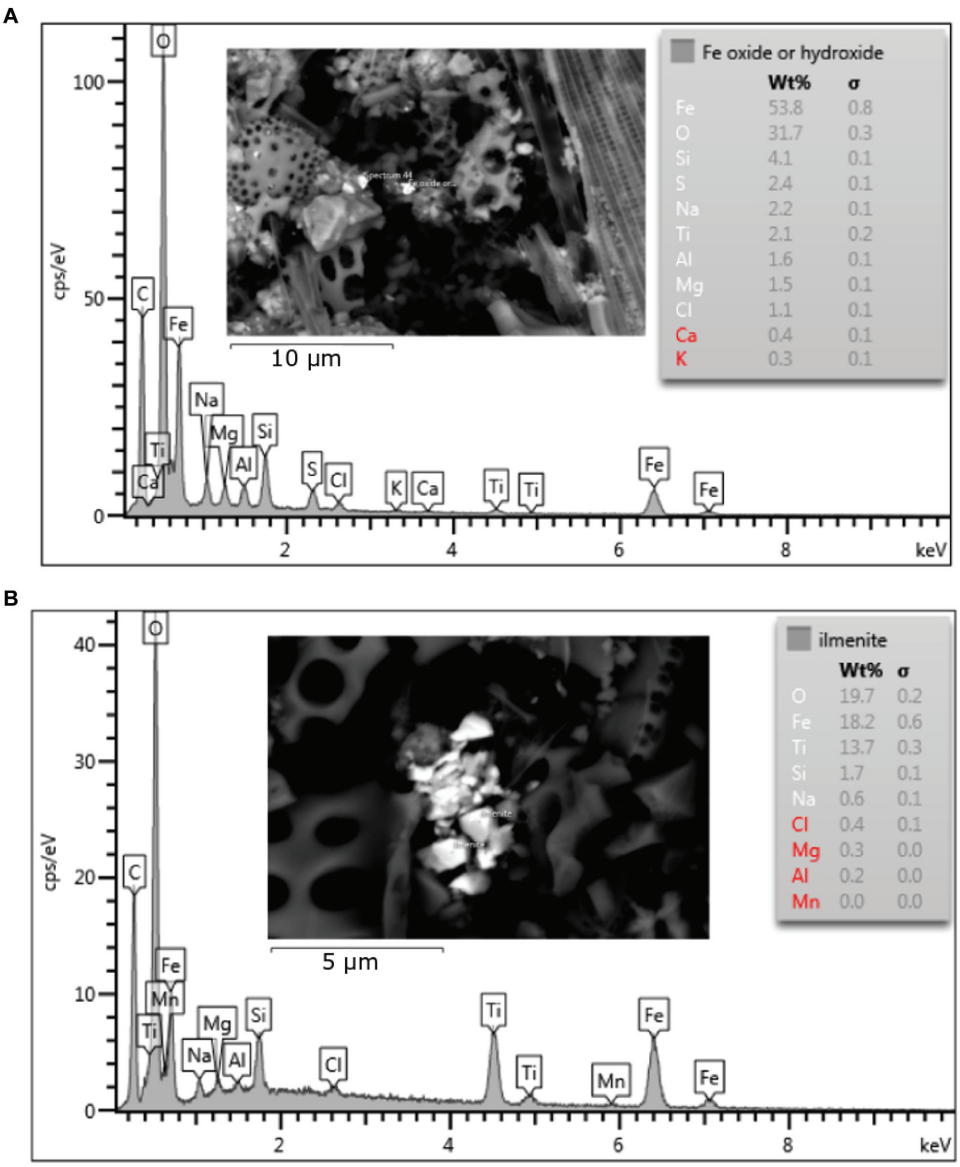

FIGURE 6 | Scanning Electron Microscope images and associated Energy-dispersive X-ray spectroscopy (EDS) spectrums showing elemental composition of the particles targeted. The spectra are representative of the particles inferred to be Fe oxyhydroxides **(A)** or ilmenite **(B)**. Red highlighted elements indicate uncertain identification.

all trace metals for downstream waters is principally derived from Heard Island.

Total particulate Fe (labile + refractory) is plotted above transmissometer data from Heard (stations ISP8, 9, and 11) and McDonald Island (stations ISP5, 6, and 10) in **Figure 10**. A higher light transmittance (percentage) equates to less particles in the water column. At Heard Island (especially stations ISP8 and 11), suspended particles and total pFe were generally higher in surface waters. Conversely, at McDonald Island (stations ISP5, 6, and 10), suspended particles and total pFe were generally lower in surface waters. It should be noted that this result is not due to variability in chlorophyll fluorescence (which is typically proportional to phytoplankton biomass) which was similar at all near shore stations, and slightly higher in surface waters at ISP10, McDonald Island.

DISCUSSION

High Fe Lability of Particles Sourced From Heard Island

Very high concentrations of labile pFe were observed at Heard Island compared to all other stations during this study. Suspended particles collected within the mixed-layer at Heard Island had significantly higher lability (pFe_{lab} = 21.5 ± 4.2%, n = 9) compared to McDonald Island (pFe_{lab} = 12.1 ± 1.1%, n = 8)

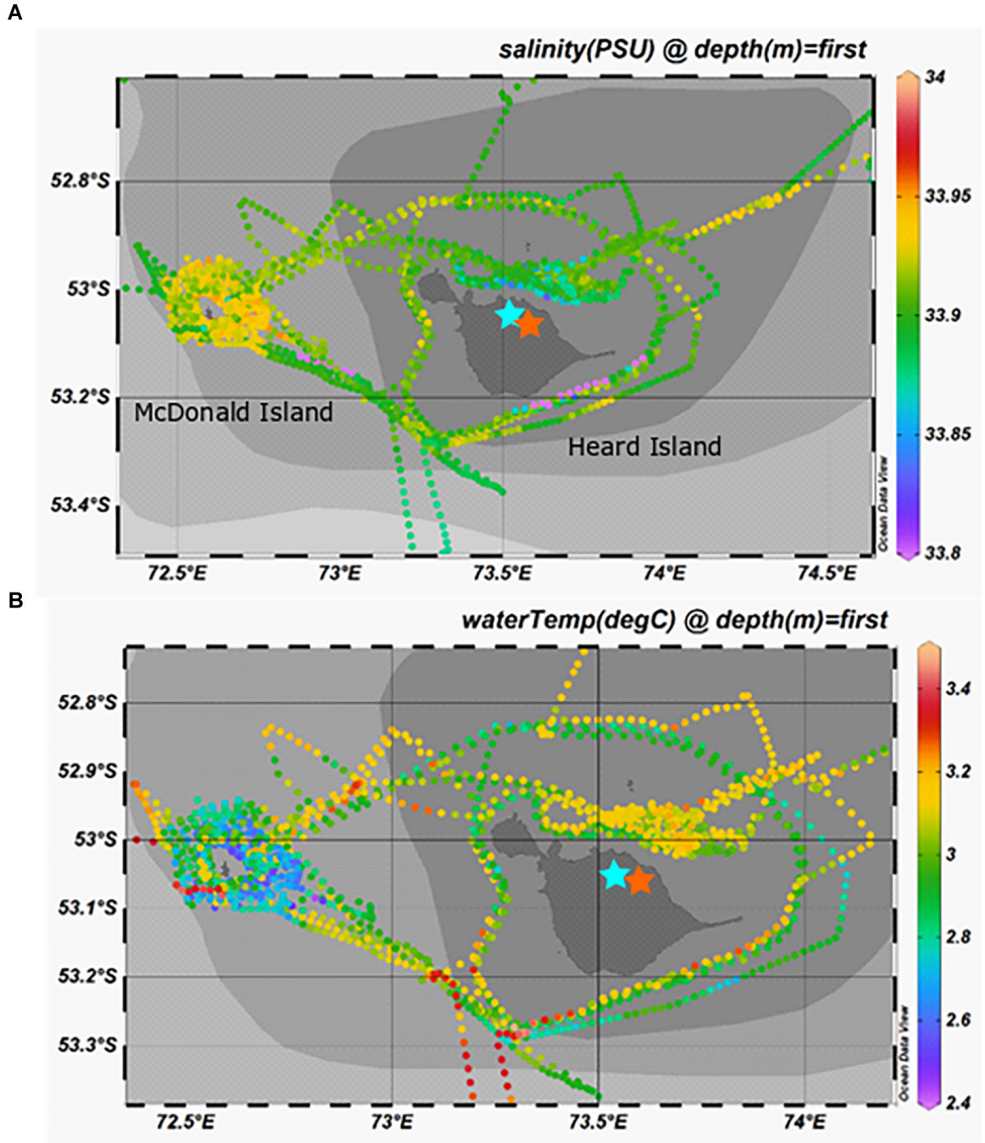

FIGURE 7 | Surface salinity **(A)** and temperature **(B)** taken from the underway sensors during the voyage. Note the parcel of fresh (aqua-blue) surface waters to the north of Heard Island, directly adjacent to outflow of Downes (blue star) and Ealey (orange star) marine terminating glaciers.

(one-way ANOVA, $p < 0.01$). Here we investigate what could cause this difference between islands that are separated by only 43 km. EDS and SEM of particles sourced from HIMI revealed that although the highly refractory Ti and Fe bearing mineral ilmenite was found commonly within the suspended particles across both islands, so too were Fe oxides and/or hydroxides (**Figure 6**). SEM-EDS is non-quantitative when used on an un-polished surface such as the filtered material in the present study, so direct comparison of abundances was not possible. Fe oxides and hydroxides have previously been found associated with icebergs and glacial ice (Raiswell et al., 2006, 2008; Hawkings et al., 2014; Markussen et al., 2016) and their lability is highly variable based on their mineralogy and age. Fe oxyhydroxide nanoparticles can be produced via sub-glacial erosion, that produces supersaturated solutions of Fe with many crystal nuclei (Raiswell et al., 2008). Likewise, hydrothermal processes, through fluid-rock chemical weathering at high temperature and low pH, can efficiently dissolve trace metals from bedrock, which upon entering oxygenated seawater, rapidly precipitate to form fine hydroxide or sulphide particles (Feely et al., 1996). Low chemical lability can be expected of minerals with lattice and covalent bonds. Conversely, higher chemical lability can be expected of minerals with ionic bonds or if the trace metal ions are bound as impurities on the surface of other minerals (Journet et al., 2008). Ilmenite, which was ubiquitous through the samples, has a highly ordered crystalline structure and as such, is highly refractory. We see this refractory nature in the relatively low mean pFe_{lab} fraction within the water column near McDonald

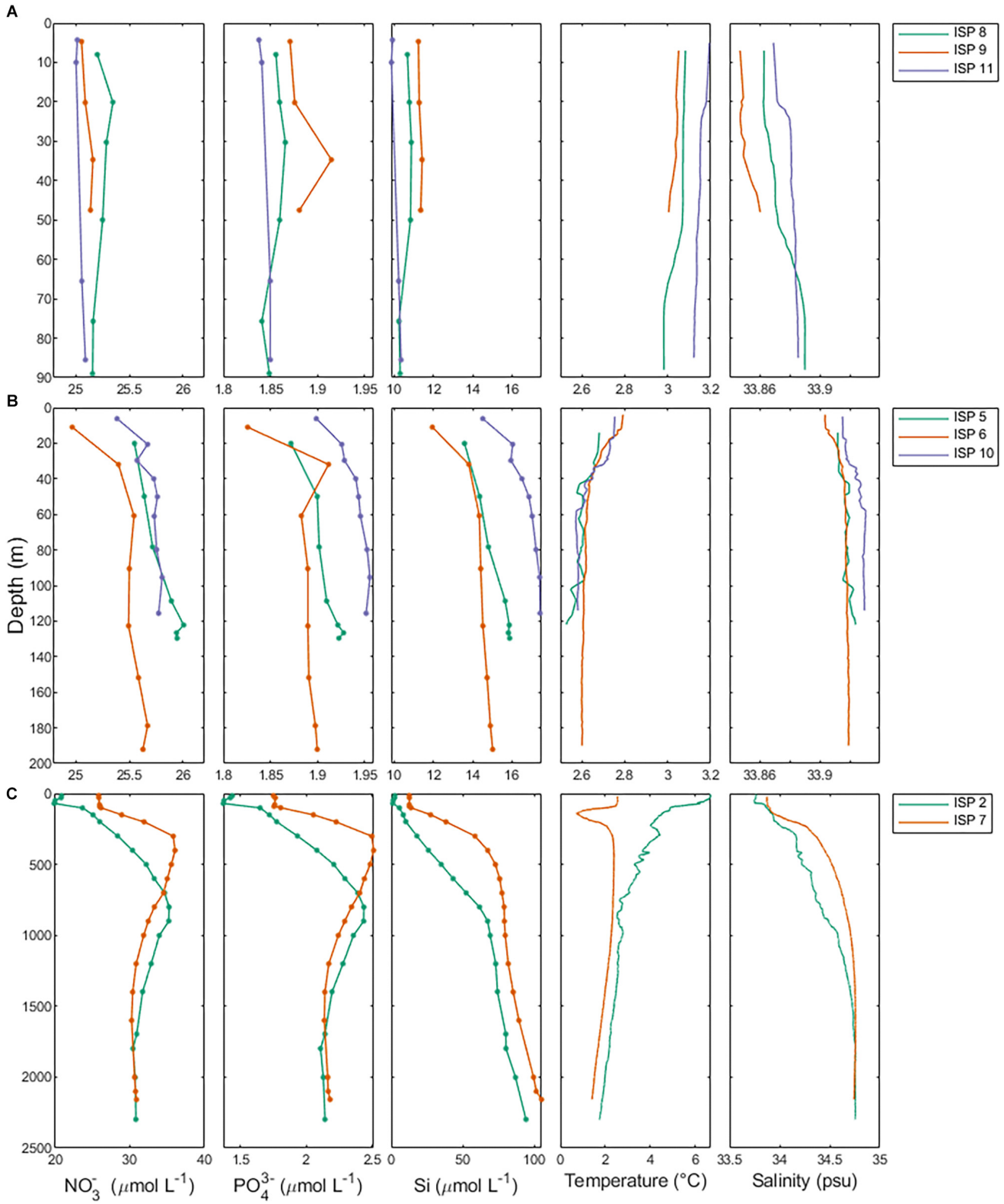

FIGURE 8 | Macronutrient, temperature and salinity profiles separated by study region. Row A (ISP8, 9, and 11) is Heard Island, row B (ISP5, 6, and 10) is McDonald Island and row C (ISP2 and 7) are the reference stations.

TABLE 5 | Spearman's ρ rank correlation coefficients, significance, and the number of independent data points used for each measurement for various parameters correlated with salinity.

Spearman's ρ rank correlation with salinity		Silicate	Nitrite	NO_X	Phosphate	dFe	pFe (refractory)	pFe (labile)
Reference	Corr. coefficient	0.906**	−0.879**	0.841**	0.841**	0.732**	0.104	0.529*
	Sig. (two-tailed)	0.000	0.000	0.000	0.000	0.001	0.713	0.043
	N	16	16	16	16	16	15	15
Plateau	Corr. coefficient	0.946**	−0.748**	0.818**	0.827**	0.801**	0.382	0.768**
	Sig. (two-tailed)	0.000	0.002	0.000	0.000	0.001	0.197	0.002
	N	14	14	14	14	14	13	13
McDonald	Corr. coefficient	0.835**	−0.913**	0.735**	0.409	0.075	0.608*	0.586*
	Sig. (two-tailed)	0.001	0.000	0.006	0.187	0.818	0.036	0.045
	N	12	12	12	12	12	12	12
Heard	Corr. coefficient	−0.698*	0.347	−0.303	−0.857**	−0.916**	0.185	−0.277
	Sig. (two-tailed)	0.037	0.360	0.429	0.003	0.001	0.634	0.470
	N	9	9	9	9	9	9	9

Salinity was taken from the CTD package on the TMR and linearly interpolated to match depths of the other parameters, therefore sample numbers represent the number of ISP samples. Asterisk indicate significance at 0.01 (**) and 0.05 (*) confidence intervals (two-tailed).

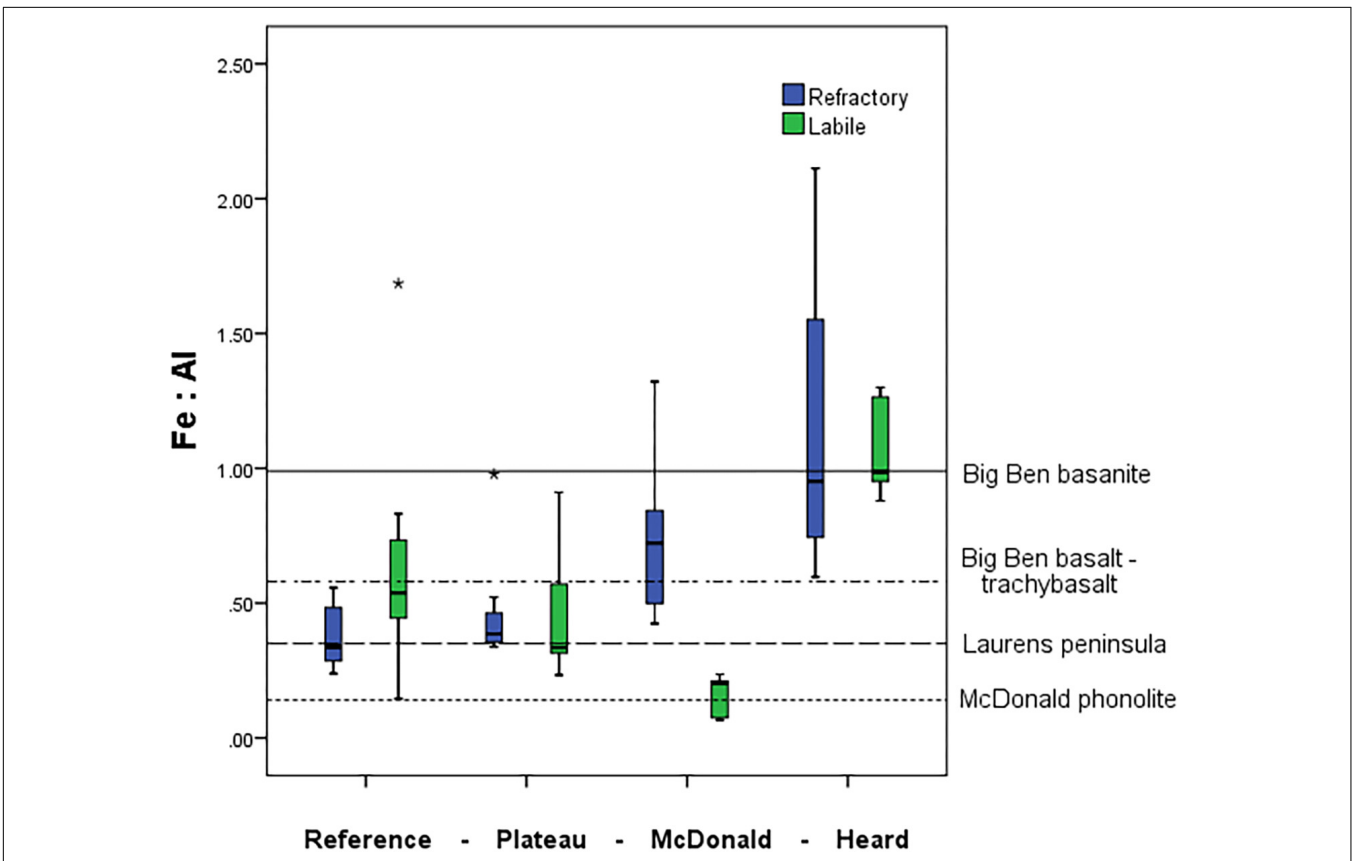

FIGURE 9 | Mean water column pFe:pAl molar ratio at the four contrasting regions within the study. Boxplots represent the labile particulate fraction in green and the refractory fraction in blue. Mean Fe:Al in rock samples from HIMI shown as horizontal lines from Barling et al. (1994). Big Ben basanite and basalt-trachybasalt was collected from several fresh lava flows around central Heard Island, while the samples from Laurens Peninsula were collected on the north-western peninsula of Heard Island. McDonald phonolite samples were collected from fresh lava flows on McDonald Island (Barling et al., 1994). Standard boxplot median (centre black line), 25th and 75th percentiles (upper and lower box limits) and 95% confidence intervals (inner fences) are indicated. Outliers are shown as circles (<1.5 × the interquartile range) and asterisk (>1.5 × the interquartile range). The number of independent data points for the reference, plateau, McDonald and Heard regions were 13, 13, 12, and 9 for pFe_{lab} and 7, 8, 12, and 9 for refractory pFe, respectively.

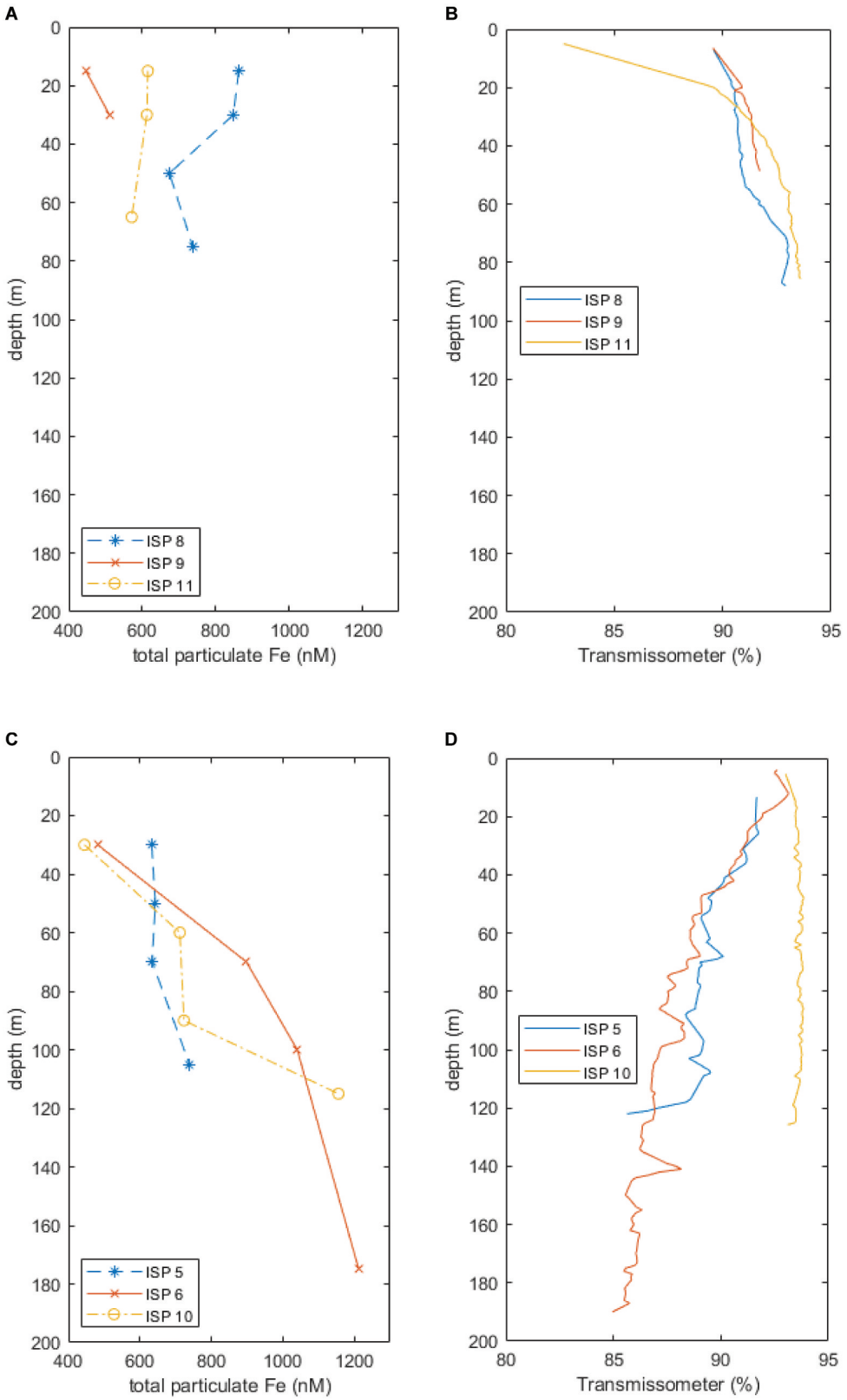

FIGURE 10 | Total particulate Fe (labile + refractory) plotted alongside transmissometer data at Heard (**A,B**, respectively) and McDonald (**C,D**, respectively) Islands. Lower light transmittance implies more suspended material in the water column. Note the contrasting trends of increasing pFe and suspended particles with depth at McDonald Island versus generally decreasing pFe and suspended particles with depth at Heard Island.

Island (**Figure 3A**). In contrast, we observed significantly higher labile Fe fractions near Heard Island. A higher proportion of Fe oxyhydroxide nanoparticles at Heard Island could explain this increase in Fe lability (Poulton and Raiswell, 2005).

Previous studies have shown that 100% of fresh (short weathering duration), poorly ordered, Fe oxyhydroxides such as 2-line ferrihydrite can be dissolved with an ascorbic acid extraction, which is indicative of relatively high chemical lability (Raiswell et al., 2010). The addition of a reductant such as dithionite increases the chemical lability of aged 2-line ferrihydrite (Raiswell, 2011) by further accessing oxyhydroxide particles, and is comparable with the Berger et al. (2008) leach used here. This suggests that relatively fresh Fe oxyhydroxides will certainly be included in this leached component, and that some aged oxyhydroxides with limited immediate bioavailability may also be included. However, as dewatering of Fe oxyhydroxides progresses through the ageing process, the rate of dissolution decreases exponentially (Raiswell et al., 2010). Therefore, it is likely that the Fe oxyhydroxides that we observed within glacial outflow, 3–7 km from Heard Island were relatively fresh, leading to the higher chemical lability we observed, in comparison to particles collected off plateau, downstream of the islands. In summary, both hydrothermalism and sub-glacial erosion/outflow have the potential to produce Fe oxyhydroxide particles which were observed at both Island locations. While the total concentration of particulate trace metals was generally higher at McDonald Island stations, pFe_{lab} was higher at Heard Island stations, suggesting either varied source rock signature, a higher proportion of Fe oxyhydroxide particles and/or modifications due to authigenic weathering processes.

The Fe:Al ratios of suspended particles observed in the water column are similar to the source rock. Previous geochemical studies have noted the stark contrast between the phonolitic lavas on McDonald and the basanite-alkali basalt-trachyte series of Heard Island (Barling et al., 1994; Quilty and Wheller, 2000). This difference in rock type is evident in the pFe:pAl molar ratio of suspended particles near these islands, which is significantly different (one-way ANOVA, $p < 0.01$) between Heard and McDonald Island (**Figure 9**). If we investigate this result further by splitting the data, we see that it is the labile particulate trace metals that drive this difference, with the refractory particulate trace metals not significantly different between Heard and McDonald Islands while the labile pFe:pAl fraction is significantly higher at Heard Island (one-way ANOVA, Games-Howell *post hoc* test, $p < 0.01$). In contrast, the reference and plateau stations do not have a significantly different pFe:pAl ratio, nor do the plateau and McDonald Island when considering only the refractory fraction. A large part of this result is due to the very high labile particulate Al (604 ± 382 nM, $n = 12$) observed at McDonald Island, which is significantly higher than at Heard Island (105 ± 16 nM, $n = 9$) (one-way ANOVA, $p < 0.01$). The high concentration of labile Al observed at McDonald may be due to the presence of glassy lavas also identified by SEM EDS in McDonald samples that have quenched in seawater before stable geochemical bonds are able to form between Si, O, and Al and therefore, can quickly erode into labile clays (Fox et al., 2017). However, the pFe_{lab} is still significantly higher at Heard, despite the higher total pFe concentration at McDonald Island. Therefore, irrespective of the high labile Al observed at McDonald Island, pFe_{lab} was independently, unusually high at Heard Island. Although only limited samples were available for this analysis, underlying sediments at nearby, but not coincident locations, mirrored the results observed in the water column with sediments at McDonald displaying a lower Fe:Al molar ratio compared to Heard Island (0.17, $n = 1$ and 1.0 ± 0.36, $n = 3$, respectively). In a separate study, whole rock samples were analysed for chemical composition. The rock samples were taken from coastal stations near HIMI, but again are not coincident with ISP stations. Despite the spatial separation of the samples, the analyses revealed mean Fe:Al molar ratios of 0.18 ± 0.05 ($n = 5$) and 0.69 ± 0.14 ($n = 7$) for McDonald and Heard Islands, respectively (Fox et al., 2017). Therefore, the Fe:Al ratios of suspended particles observed in the water column were approximately as expected from direct weathering of the source rock.

What Evidence Supports Glacial/Fluvial Supply at Heard Island?

A source of fresh surface water was observed near the outflowing glacier to the north of Heard Island (**Figure 7**). The change in salinity was small (∼0.05) but it is distinct compared to other measurements taken around the islands. We also observed low salinity surface waters to the southeast, downstream of Heard Island. The full water column salinity and temperature profiles at Heard Island although quite well mixed, are fresher and warmer than at McDonald Island (**Figure 8**). Glacial meltwater outflow may explain this low salinity coastal water. Indeed, over the full water column, salinity correlated inversely with dFe, silicate and phosphate at Heard Island only (**Table 5**). Interestingly, no such correlation was observed for particulate Fe highlighting the complexity of particle supply across a salinity gradient and into a highly turbulent coastal environment. We suggest that this glacial source is supplying Fe in both the dissolved and particulate fractions, however, the complex removal and settling processes may affect the particulate and dissolved fractions in different ways (Zhang et al., 2015). It is important to note in this context that nanoparticulate Fe oxyhydroxides within the colloidal phase would pass through 0.2 μm filtration if present and thus be included in the operationally defined dissolved phase and may have a bearing on our observed correlation between fresh water and the "dissolved phase." For this reason, the dissolved phase may better be defined as colloidal/nanoparticulate Fe (CNFe) (Raiswell et al., 2018). Extrapolating the Heard Island salinity correlations of dissolved silicate, phosphate and dFe to the freshwater endmember suggests concentrations above seawater of ∼1092 ± 188 μM, 38 ± 7.4 μM and 548 ± 93 nM, respectively. This level of dissolved silicate enrichment is approximately sixfold higher than in rivers globally (158 μM) (Dürr et al., 2011), and approximately fivefold higher than maximum observations in the Antarctic ice sheet meltwater (130–210 μM) (Michaud et al., 2016) and closer to levels of amorphous Si observed in Greenlandic glacier meltwaters (120–627 μM) (Hawkings et al., 2017). This implies a non-conservative supply of silicate, possibly

from amorphous Si particles transported offshore together with meltwater and subsequent dissolution, and possibly from resuspension and biotic dissolution of Si rich diatom frustules (Bidle and Azam, 1999) [SEM analysis revealed very high relative proportions (∼90%) of diatom frustules in the suspended particles around both islands (**Figure 6**)]. The implied phosphate enrichment is higher than expected [rivers generally have lower phosphate than deep seawater unless they derive from fertilised catchments, (Martin and Meybeck, 1979)]. The endmember dFe concentration agrees well with previous observations in glacial meltwater rivers [e.g., 734 nM in the Bayelva River near a glacier in Svalbard (Zhang et al., 2015) or 200–9,000 nM range in multiple Greenlandic glacier fed rivers (Raiswell et al., 2018)]. While the standard error on these regressions is large, this suggests that the association of enhanced nutrient levels with lower salinity near Heard Island may involve multiple mechanisms. Sub-glacial discharge is the most likely source of the fresh water, and presumably arrives laden with dFe, silicate, amorphous Si and other particles. Sediment resuspension by the momentum of the cascades of freshwater inflows and strong tidal currents (Maraldi et al., 2009), as well as phosphate-rich guano from the abundant bird life, are possible sources of the nutrient enrichments (Pakhomov and Froneman, 1999).

While stationed at site 9 in front of Downes and Ealey marine terminating glaciers, we noticed the characteristic milky discolouration of glacial flour suspension within the surface waters, while at the same time, Wojtasiewicz et al. (n.d) observed a very high proportion of non-phytoplankton small particles via *in situ* bio-optical profiling measurements. This anomaly in the bio-optical measurements was likely glacial flour suspended in the water column and potentially reduced photosynthetically active radiation to limiting levels in coastal waters (Wojtasiewicz et al., n.d). In contrast to McDonald Island, at Heard Island, the transmissometer profiles and particulate Fe through the water column were generally higher in the surface waters (**Figure 10A**), indicative of Fe enriched, low-density, fresh-water supply from glacial/fluvial sources. Furthermore, satellite imagery of Heard Island revealed a sharp delineation between outflowing sediment laden water and the surrounding coastal waters (**Figure 2A**), which is seen to the north and north east of Heard Island. The sharp delineation is characteristic of point source outflow such as glacial meltwater or fluvial outflow. Interestingly, the eruption on Heard Island that was occurring at the time of our occupation was causing lava to flow over the glaciers and eventually disappear after melting into the glaciers (**Figure 2B**). This active melting of the glaciers may have caused an additional input of glacial meltwater into the surrounding coastal waters during our occupation which is difficult to quantify. However, previous research has shown that the Pine Island Glacier in West Antarctica, an area known for supplying high concentrations of dissolved and total dissolvable Fe which fertilises a large downstream phytoplankton bloom (Gerringa et al., 2012), overlies a significant geothermal heat source which effects its stability and increases the production of subglacial water (Loose et al., 2018). This analogous region shows that geothermal heat can have a direct impact on the supply of trace elements in glaciated catchments. However, at Heard Island, mean daily air temperatures at sea level range from 3.7 to 5.2°C in summer and −0.8–0.3°C in winter, but above 500 m remain persistently sub-freezing (Thost and Truffer, 2008) and these warmer summer temperatures drive freeze-thaw cycles and glacial meltwater outflow during the summer months. Our occupation (January–February 2016) occurred in mid-summer and therefore, seasonal meltwater may have masked additional outflow attributed to geothermal heat.

At Heard Island, just like at the well documented Kerguelen Island, mean temperatures have risen by 0.9 degrees over the last 70 years (Thost and Truffer, 2008). Furthermore, aerial photographs from 1947, 1980 and satellite observations since, document that at Heard, some glaciers have retreated by 29% in area, corresponding in a 0.5 m a^{-1} thinning since 1947 (Allison and Keage, 1986; Budd, 2000; Thost and Truffer, 2008). Furthermore, glacier retreat has accelerated recently with estimates of ice mass loss in the early 2000s being twice the previous 57-year mean (Thost and Truffer, 2008), resulting in enhanced meltwater outflow. Therefore, as the glaciers on Heard continue to lose mass, an initial increase in sub-glacial melt water may increase the delivery of trace metals into the surrounding waters. While it is beyond the scope of this paper to predict the rate of glacial erosion into the future under a warming climate, the production of glacial flour and Fe oxyhydroxide nanoparticles appears tied to the presence of glaciers on Heard. While near shore impacts of glacial outflow are clear, how far and in what form the trace metal fertilisation extends from the coast requires further quantification.

What Evidence Supports Hydrothermal Supply at McDonald Island?

Although clear signs of subaerial volcanic activity were observed on both Heard and McDonald Islands, hydrothermal activity surrounding the islands was subtle and its impact on particulate trace metals difficult to quantify. Dissolved Fe and pFe_{lab} are positively correlated with salinity at the reference (R = 0.73, $p < 0.01$ and R = 0.53, $p < 0.05$, respectively) and plateau (R = 0.80, $p < 0.01$ and R = 0.77, $p < 0.01$, respectively) stations (**Table 5**). Silicate, NOx and both labile and refractory pFe were also correlated with salinity at McDonald Island due to all these variables increasing with depth (**Figures 8**, **10**). This contrasts with profiles near Heard Island which were generally well mixed with enrichment of total particulate Fe and dFe in surface waters leading to an inverse correlation between salinity and dFe, silicate and phosphate. For an in-depth look at the role of hydrothermalism in supplying dFe during this voyage, see Holmes et al. (n.d). Briefly, advanced sonar systems (Simrad EK60 echo sounder) onboard the Investigator were used to search for bubble plume anomalies while the ship was performing detailed bathymetric surveys around Heard and McDonald Island (Watson et al., 2016). Once a large bubble plume was identified, the underwater towed camera system was deployed to visually inspect the plumes. Although over 200 bubble plumes were found around HIMI, they were all low energy, with no detectable heat signature. Spain et al. (2018) suggested that bubble plumes emanating from thick seafloor

sediments near Heard Island, as evidenced from the sub bottom profiler images, and gas pockets within the sediments, implied methanogenesis, as has been observed at South Georgia (Römer et al., 2014). Conversely, at McDonald Island, bubble plumes were observed emanating from areas with a thin (<5 m) seafloor sediment veneer, and sometimes almost solid bedrock with domed morphologies (Watson et al., 2016) similar to what has been observed in shallow gasohydrothermal fields in Naples Harbour, Italy (Passaro et al., 2016). Indeed, Lupton et al. (2017) revealed that excess ^{3}He was observed at several of these bubble flares, particularly in the waters surrounding McDonald Island. This is clear evidence for shallow diffuse venting in these waters. This implies that methanogenesis was unlikely at McDonald Island, and that the emanating bubbles were likely to be CO_2 sourced from diffuse hydrothermal venting, although further work is required to confirm this.

Hydrothermal bubble flares and deep-water trace metal enrichment were observed near McDonald Island. When we compare particle concentration (from transmissometer data) with pFe concentrations, we see that suspended particles from ISP5, 6, and 10 near McDonald Island generally increase with depth (**Figure 10B**). Conversely, suspended particles are generally lower at depth near Heard Island (**Figure 10A**). Although seafloor sediment resuspension would be a likely candidate for this increase with depth at McDonald, sub-bottom profile images suggest that only a thin sediment veneer is present at McDonald Island (Spain et al., 2018). It is possible that diffuse venting and buoyant bubble plumes are aiding resuspension of seafloor sediments and direct supply of vent precipitates near the seafloor in the region. Methanogenesis derived bubble plumes observed near Heard Island did not seem to resuspend deep seafloor sediment in the same manner and suggests that the bubble plumes at McDonald are associated with more suspended particles. Furthermore, dissolved Fe(II), the short lived, reduced form of dissolved Fe(III), was observed at high ratios to the total dissolved pool at sites near McDonald Island that also displayed ^{3}He anomalies (Holmes et al., n.d), indicative of hydrothermal activity. Furthermore, ISP stations 10 and 6 (off the eastern coast of McDonald Island) which targeted a large bubble plume, displayed the most rapid increase toward the seafloor and highest absolute concentrations in total pFe measured during this voyage, coincident with the highest dissolved Fe(II):Fe(III) ratio (Holmes et al., n.d) and ^{3}He anomaly (Lupton et al., 2017) observed. Therefore, we conclude that evidence of shallow, diffuse hydrothermalism was detected near McDonald Island, however, to quantify the wider impact of this supply to the downstream blooms requires further investigation.

Comparison of pFe_{lab} to dFe Inventories

The concentration of pFe_{lab} is ∼100-fold higher than dFe near both Heard and McDonald Islands (**Figure 5**), with Heard showing significantly higher values of pFe_{lab} compared to McDonald (one-way ANOVA, $p < 0.01$, **Figure 3A**). Even far from the islands, over the plateau, pFe_{lab} (1.1 ± 3 nM, $n = 13$) is approximately equal to dFe (0.31 ± 0.25 nM, $n = 14$) and thus roughly triples the inventory of Fe potentially available for phytoplankton. In contrast, within the mixed layer at the reference station, pFe_{lab} (0.02 ± 0.03 nM, $n = 3$) contributes only a small fraction of the total Fe potentially available for phytoplankton (dFe + pFe_{lab} = 0.15 nM). The high concentrations of pFe_{lab} near the islands are therefore potentially a major Fe source, and only a small fraction needs be bioavailable to drive phytoplankton growth. Its overall influence depends both on its delivery downstream and on the fraction which is or can become bioavailable.

What Processes Are Important for Delivery of pFe_{lab} Into Downstream Waters?

Multiple mechanisms impact the fate of pFe_{lab} as it is transported away from the islands. It has been shown that pFe is often exported out of the mixed layer over a salinity gradient in close proximity to a source (Hawkings et al., 2014; Schroth et al., 2014), but the rates of flocculation and settling can vary strongly (Markussen et al., 2016). This sinking loss rate increases as a function of particle size and density. Stokes law predicts that the sinking rate of glacial rock flour, characteristically within the silt-clay size range, would result in sinking rates of 0.2–165 m d^{-1}, i.e., residence times varying from less than a day to more than a year (in a 100 m mixed layer). Larger higher density particles will be preferentially lost. Smaller, lower density, and potential more reactive particles such as amorphous particles (Hawkings et al., 2018) will be retained, and thus will be transported further. Thus, the initial size and density of the pFe_{lab} containing particles is important.

In addition, the interaction with marine organic matter is important. Coagulation of pFe_{lab} particles with low density particulate organic matter may help it to stay suspended in the water column, where it can be efficiently recycled via microbial processes (Boyd et al., 2017). The fate of dFe released in this way from pFe_{lab} or via abiotic dissolution can in turn be extended by Fe binding ligands, as produced *in situ* by phytoplankton and bacteria (Lis et al., 2015). This complexation reduces the rate of precipitation and thus increases the residence time of Fe in the mixed layer. During the present voyage, organic Fe binding ligands were quantified with respect to the dFe pool (Tonnard et al., n.d) and were found to be saturated with dFe near HIMI, suggesting that their availability is a possible controlling factor on Fe retention and its supply downstream. Importantly, the supply of pFe_{lab} to the ecosystem can itself stimulate processes that enhance its retention in the water column. The added iron drives production which is a source of more organic ligands, as has been observed in other glaciated catchments (Thuróczy et al., 2012; Hopwood et al., 2016).

Clearly loss by sinking is a dominant control, given that both pFe and pFe_{lab} concentrations are ∼100-fold lower at the plateau sites than near the islands. Transport of a water parcel between Heard Island and ISP3 takes ∼60 days based on an average surface current velocity of 4.0 m s^{-1} (Park et al., 2008) and therefore provides considerable time for interactions with the organic particulate and ligand pools. Thus, many aspects of pFe and pFe_{lab} properties are likely to evolve between the island sources and the regions where blooms form, including

particle sinking rates and bioavailability. Perhaps surprisingly, given the two orders of magnitude decrease in pFe and pFe_{lab} concentrations, their relative proportions varied only slightly (∼3-fold) among the sites. For samples within the mixed layer, the pFe_{lab} fraction of total pFe averaged 5 ± 9% at the plateau stations, 10 ± 15% at the reference stations, 11 ± 4% near McDonald Island, and 18 ± 6% near Heard Island. This suggests that this ratio may be set by particle associations close to the source and then only evolve slightly over time, with a slow decrease in the proportion of remaining pFe_{lab}.

Can the Flux of pFe_{lab} From Heard Island Balance Phytoplankton Demand?

Previous studies have shown that lateral advection from Heard is the dominant Fe supply route to ISP3 (previously referred to as station B3) over the plateau (Chever et al., 2010) linking this large supply directly to the downstream blooms. The involvement of pFe in sustaining the spring bloom in the region has been hypothesised before. Several studies have attempted to account for all the sources and sinks including remineralisation of Fe within a system and have compared this to the measured phytoplankton demand. Blain et al. (2007) concluded that to close the Fe budget calculated for the Kerguelen plateau during the 2005 KEOPS-1 voyage, phytoplankton must be able to access around 2.5% of the pFe pool. Bowie et al. (2015) extended the Fe budget for the region and also noted a deficit between supply of Fe and the measured phytoplankton demand, and again pointed to the particulate fraction as the most likely source.

Our measurements of pFe_{lab} provide a new estimate of the portion of pFe that may potentially become available for phytoplankton consumption. For samples within the mixed layer over the plateau this ranged from 5 to 18% (see previous section for details) and thus was sufficient to at least supplement the dFe pool. This further emphasises the ability of Fe derived from particles to contribute to and sustain phytoplankton blooms.

Calculation of the delivery of pFe and pFe_{lab} from their island sources to the plateau is difficult, because we do not know their loss rates by sinking or how they evolve along the trajectory [this sinking loss term overwhelms all other input and removal terms, as well as conversions among dissolved and particulate pools as shown by the more complete box model of Chever et al. (2010)]. Using the following first order exponential over the approximately 60-day transit, an average sinking loss rate of 7% per day is low enough to retain pFe and pFe_{lab} within the mixed layer and deliver the observed concentrations over the plateau.

$$I^{(t)} = I^0 e^{-\frac{d}{1/pFe_{loss}}}$$

Where $I^{(t)}$ is the integrated stock of pFe_{lab} at time (t), I^0 is the mean integrated initial stock of pFe_{lab} at time 0 at Heard, d is the transport duration in days, and pFe_{loss} is the mean vertical loss rate per day of total pFe from the mixed layer.

This 7% per day loss rate seems plausible: data published in van der Merwe et al. (2015) documented a 70% loss of total pFe from the mixed layer over 27 days at station A3 over the plateau, due to the development of a phytoplankton bloom, equating to a loss rate of 3.4% per day; and dividing A3 pFe mixed layer standing stocks by the pFe fluxes collected using sediment traps deployed at A3 for this same 27-day-period (Bowie et al., 2015) suggests a vertical loss rate of 1.2% per day.

In summary, the observed amounts are sufficient and the timescales for delivery are appropriate for pFe_{lab} derived from McDonald and especially Heard Island sources to sustain the necessary Fe budgets to drive formation of the phytoplankton blooms that form over the Kerguelen plateau.

CONCLUSION

McDonald Island is almost completely ice free, while Heard Island is almost entirely covered by glaciers and snow. Simultaneously, the rock types on these islands are also unique in terms of their elemental composition. Suspended particles near Heard Island were significantly more labile than at McDonald Island (21.5 ± 4.2%, n = 9 and 11.6 ± 1.3%, n = 12, respectively). It is likely that the Fe oxyhydroxides that we observed within glacial outflow near Heard Island were relatively fresh, leading to the higher chemical lability we observed, in comparison to highly refractory minerals such as ilmenite collected ubiquitously around both islands. High pFe:pAl suspended particles found in the present study, directly adjacent to glacial outflow, highlight the contrasting rock types found on Heard and McDonald Island, but authigenic processes during sub-glacial erosion may also play a part in modifying this ratio. The source water for fertilisation of dFe (potentially including nanoparticulate Fe oxyhydroxides), silicate and phosphate at Heard Island is fresh, and glacial and fluvial outflow are likely sources of this fertilisation. Conversely, pFe (>0.4 μm) did not correlate with salinity, highlighting the previously documented complex removal and sedimentation processes that occur over a salinity gradient. At other regions, fertilisation is linked with higher salinity deep-water, suggesting an alternate source. The role of diffuse venting in supply of particulate material at McDonald Island seems likely, with multiple complimentary data sets pointing to a hydrothermal source of pFe, pFe_{lab} and dFe at this location. Large scale quantification of this hydrothermal source requires further work but given that McDonald Island is two orders of magnitude smaller in surface area than Heard Island, we predict this to be minor compared to the glacial/fluvial sources on Heard Island. Our results show that pFe_{lab} can act as a vector for Fe transport downstream of the Islands into waters with sufficient organic ligands to complex further Fe supply as it becomes available through biotic and abiotic dissolution. Our calculations provide good evidence that the pFe_{lab} supplied from Heard and to a lesser extent, McDonald Island, is indeed the missing Fe required to meet demand over the plateau, downstream of the islands where traditionally an intense bloom develops in spring and summer.

DATA AVAILABILITY

All datasets generated for this study are included in the manuscript and/or the supplementary files.

AUTHOR CONTRIBUTIONS

PvdM collected, processed, and analysed the samples, interpreted the results, and prepared the manuscript. KW, TT, TH, ZC, and AB assisted in sampling. KW also did processing and analyses. AT ran the ICPMS instrumentation. KG instructed PV and KW on SEM EDS analysis and aided in interpretation of that data. All co-authors contributed suggestions and refinements to the manuscript.

FUNDING

This work was funded by the Australian Research Council Discovery (DP150100345) and Australian Antarctic Science (AAS4338) grants, and the Australian Commonwealth Government through the Antarctic Climate and Ecosystem Co-operative Research Centre. Access to sector-field inductively coupled plasma-mass spectroscopy and scanning electron microscopy instrumentation was supported through the Australian Research Council, Linkage Infrastructure, Equipment and Facilities funding (LE0989539 and LE100100107, respectively).

ACKNOWLEDGMENTS

We thank the officers and crew of the RV Investigator and staff at the Marine National Facility for their help and support before, during, and after the cruise. We thank the chief scientist, Mike Coffin for design and implementation of this research voyage. We also thank Brett Muir as voyage manager. Discussions with Erica Spain and Jodi Fox were very valuable in interpreting bubble plumes and Heard and McDonald Island geology, respectively.

REFERENCES

Allison, I. F., and Keage, P. L. (1986). Recent changes on the glaciers of heard island. *Polar Rec.* 23, 255–272. doi: 10.1017/S0032247400007099

Appelblad, P. K., Rodushkin, I., and Baxter, D. C. (2000). The use of Pt guard electrode in inductively coupled plasma sector field mass spectrometry: advantages and limitations. *J. Anal. At. Spectrom.* 15, 359–364. doi: 10.1039/a906531h

Arrigo, K. R., van Dijken, G. L., and Strong, A. (2015). Environmental controls ofmarine productivity hot spots around Antarctica. *J. Geophys. Res. Oceans* 120, 5545–5565. doi: 10.1002/2015JC010888.Received

Barling, J., Goldstein, S. L., and Nicholls, I. A. (1994). Geochemistry of heard Island (Southern Indian Ocean): Characterization of an enriched mantle component and implications for enrichment of the sub-Indian ocean mantle. *J. Petrol.* 35, 1017–1053. doi: 10.1093/petrology/35.4.1017

Berger, C. J. M., Lippiatt, S. M., Lawrence, M. G., and Bruland, K. W. (2008). Application of a chemical leach technique for estimating labile particulate aluminum, iron, and manganese in the Columbia River plume and coastal waters off Oregon and Washington. *J. Geophys. Res.* 113, 1–16. doi: 10.1029/2007JC004703

Bidle, K. D., and Azam, F. (1999). Accelerated dissolution of diatom silica by marine bacterial assemblages. *Nature* 397, 508–512. doi: 10.1038/17351

Bishop, J. K. B., Lam, P. J., and Wood, T. J. (2012). Getting good particles: accurate sampling of particles by large volume in-situ filtration. *Limnol. Oceanogr. Methods* 10, 681–710. doi: 10.4319/lom.2012.10.681

Blain, S., Queguiner, B., Armand, L., Belviso, S., Bombled, B., Bopp, L., et al. (2007). Effect of natural iron fertilization on carbon sequestration in the Southern Ocean. *Nature* 446, 1070–1074. doi: 10.1038/nature05700

Bowie, A. R., Townsend, A. T., Lannuzel, D., Remenyi, T. A., and van der Merwe, P. (2010). Modern sampling and analytical methods for the determination of trace elements in marine particulate material using magnetic sector inductively coupled plasma-mass spectrometry. *Anal. Chim. Acta* 676, 15–27. doi: 10.1016/j.aca.2010.07.037

Bowie, A. R., Van Der Merwe, P., Queroue, F., Trull, T., Fourquez, M., Planchon, F., et al. (2015). Iron budgets for three distinct biogeochemical sites around the Kerguelen Archipelago (Southern Ocean) during the natural fertilisation study, KEOPS-2. . *Biogeosciences* 12, 4421–4445. doi: 10.5194/bg-12-4421-2015

Boyd, P. W., and Ellwood, M. J. (2010). The biogeochemical cycle of iron in the ocean. *Nat. Geosci.* 3, 675–682. doi: 10.1038/ngeo964

Boyd, P. W., Ellwood, M. J., Tagliabue, A., and Twining, B. S. (2017). Biotic and abiotic retention, recycling and remineralization of metals in the ocean. *Nat. Geosci.* 10, 167–173. doi: 10.1038/ngeo2876

Browning, T. J., Stone, K., Bouman, H. A., Mather, T. A., Pyle, D. M., Moore, C. M., et al. (2015). Volcanic ash supply to the surface ocean - remote sensing of biological responses and their wider biogeochemical significance. *Front. Mar. Sci.* 2:14. doi: 10.3389/fmars.2015.00014

Budd, G. (2000). Changes in Heard Island glaciers, king penguins and fur seals since 1947. *Pap. Proc. R. Soc.* 133, 47–60. doi: 10.26749/rstpp.133.2.47

Chever, F., Sarthou, G., Bucciarelli, E., Blain, S., and Bowie, A. R. (2010). An iron budget during the natural iron fertilisation experiment KEOPS (Kerguelen Islands, Southern Ocean). *Biogeosciences* 7, 455–468. doi: 10.5194/bg-7-455-2010

de Baar, H. J. W., Boyd, P. W., Coale, K. H., Landry, M. R., Tsuda, A., Assmy, P., et al. (2005). Synthesis of iron fertilization experiments: from the Iron Age in the Age of Enlightenment. *J. Geophys. Res.* 110:C09S16. doi: 10.1029/2004JC002601

de Boyer Montégut, C., Madec, G., Fischer, A. S., Lazar, A., and Iudicone, D. (2004). Mixed layer depth over the global ocean: an examination of profile data and a profile-based climatology. *J. Geophys. Res.* 109:C12003. doi: 10.1029/2004JC002378

Dürr, H. H., Meybeck, M., Hartmann, J., Laruelle, G. G., and Roubeix, V. (2011). Global spatial distribution of natural riverine silica inputs to the coastal zone. *Biogeosciences* 8, 597–620. doi: 10.5194/bg-8-597-2011

Feely, R. A., Baker, E. T., Marumo, I. K., Urabe, T., Ishibashl, J., Gendron, J., et al. (1996). Hydrothermal plume particles and dissolved phosphate over the superfast-spreading southern East Pacific Rise. *Geochim. Cosmochim. Acta* 60, 2297–2323. doi: 10.1016/0016-7037(96)00099-3

Fitzsimmons, J. N., Boyle, E. A., and Jenkins, W. J. (2014). Distal transport of dissolved hydrothermal iron in the deep South Pacific Ocean. *Proc. Natl. Acad. Sci. U.S.A.* 111, 16654–16661. doi: 10.1073/pnas.1418778111

Fox, J. M., Carey, R. J., Coffin, M. F., Watson, S. J., Olin, P., Arculus, R. et al. (2017). McDonald Islands – An example of submarine and subaerial phonolitic volcanism on the Kerguelen Plateau, the southern Indian Ocean, Abstracts of the IAVCEI Scientific Assembly, Fostering Integrative Studies of Volcanoes, Abstract 714, 714.

Gartman, A., Findlay, A. J., and Luther, G. W. (2014). Nanoparticulate pyrite and other nanoparticles are a widespread component of hydrothermal vent black smoker emissions. *Chem. Geol.* 366, 32–41. doi: 10.1016/j.chemgeo.2013.12.013

Gerringa, L. J. A., Alderkamp, A.-C., Laan, P., Thuróczy, C.-E., de Baar, H. J. W., Mills, M. M., et al. (2012). Iron from melting glaciers fuels the phytoplankton blooms in Amundsen Sea (Southern Ocean): Iron biogeochemistry. *Deep Sea Res. Part II Top. Stud. Oceanogr.* 71–76, 16–31. doi: 10.1016/j.dsr2.2012.03.007

Hawkings, J. R., Benning, L. G., Raiswell, R., Kaulich, B., Araki, T., Abyaneh, M., et al. (2018). Biolabile ferrous iron bearing nanoparticles in glacial sediments. *Earth Planet. Sci. Lett.* 493, 92–101. doi: 10.1016/j.epsl.2018.04.022

Hawkings, J. R., Wadham, J. L., Benning, L. G., Hendry, K. R., Tranter, M., Tedstone, A., et al. (2017). Ice sheets as a missing source of silica to the polar oceans. *Nat. Commun.* 8:14198. doi: 10.1038/ncomms14198

Hawkings, J. R., Wadham, J. L., Tranter, M., Raiswell, R., Benning, L. G., Statham, P. J., et al. (2014). Ice sheets as a significant source of highly reactive nanoparticulate iron to the oceans. *Nat. Commun.* 5:3929. doi: 10.1038/ncomms4929

Herraiz-Borreguero, L., Lannuzel, D., van der Merwe, P., Treverrow, A., and Pedro, J. B. (2016). Large flux of iron from the Amery Ice Shelf marine ice to Prydz Bay, East Antarctica. *J. Geophys. Res.* 121, 6009–6020. doi: 10.1002/2016JC011687

Holmes, T. M., Chase, Z., Van Der Merwe, P., Townsend, A. T., and Bowie, A. R. (2017). Detection, dispersal and biogeochemical contribution of hydrothermal iron in the ocean. *Mar. Freshw. Res.* 68, 2184–2204. doi: 10.1071/MF16335

Holmes, T. M., Wuttig, K., Chase, Z., van der Merwe, P., Townsend, A. T., Schallenberg, C., et al. (2019). Iron availability influences nutrient drawdown in the Heard and McDonald Islands region, Southern Ocean. *Mar. Chem.* 211, 1–130. doi: 10.1016/J.MARCHEM.2019.03.002

Holmes, T. M., Wuttig, K., Chase, Z., Schallenberg, C., van der Merwe, P., Townsend, A. T., et al. (n.d). Glacial and hydrothermal sources of dissolved iron(II) in Southern Ocean waters surrounding Heard and McDonald Islands.

Hopwood, M. J., Bacon, S., Arendt, K., Connelly, D. P., and Statham, P. J. (2015). Glacial meltwater from Greenland is not likely to be an important source of Fe to the North Atlantic. *Biogeochemistry* 124, 1–11. doi: 10.1007/s10533-015-0091-6

Hopwood, M. J., Connelly, D. P., Arendt, K. E., Juul-Pedersen, T., Stinchcombe, M. C., Meire, L., et al. (2016). Seasonal Changes in Fe along a Glaciated Greenlandic Fjord. *Front. Earth Sci.* 4:15. doi: 10.3389/feart.2016.00015

Hopwood, M. J., Statham, P. J., Tranter, M., and Wadham, J. L. (2014). Glacial flours as a potential source of Fe(II) and Fe(III) to polar waters. *Biogeochemistry* 118, 443–452. doi: 10.1007/s10533-013-9945-y

Journet, E., Desboeufs, K. V., Caquineau, S., and Colin, J. L. (2008). Mineralogy as a critical factor of dust iron solubility. *Geophys. Res. Lett.* 35, 3–7. doi: 10.1029/2007GL031589

Lam, P. J., Ohnemus, D. C., and Marcus, M. A. (2012). The speciation of marine particulate iron adjacent to active and passive continental margins. *Geochim. Cosmochim. Acta* 80, 108–124. doi: 10.1016/j.gca.2011.11.044

Lannuzel, D., Schoemann, V., de Jong, J. T., Pasquer, B., van der Merwe, P., Masson, F., et al. (2010). Distribution of dissolved iron in Antarctic sea ice: spatial, seasonal, and inter-annual variability. *J. Geophys. Res* 115, 134–146. doi: 10.1029/2009JG001031

Lannuzel, D., Vancoppenolle, M., van der Merwe, P., de Jong, J., Meiners, K. M., Grotti, M., et al. (2016). Iron in sea ice: review and new insights. *Elementa* 4:000130. doi: 10.12952/journal.elementa.000130

Lis, H., Shaked, Y., Kranzler, C., Keren, N., and Morel, F. M. M. (2015). Iron bioavailability to phytoplankton: an empirical approach. *ISME J.* 9, 1003–1013. doi: 10.1038/ismej.2014.199

Loose, B., Garabato, A. C. N., Schlosser, P., Jenkins, W. J., Vaughan, D., and Heywood, K. J. (2018). Evidence of an active volcanic heat source beneath the Pine Island Glacier. *Nat. Commun.* 9:2431. doi: 10.1038/s41467-018-04421-3

Lupton, J. E., Arculus, R. J., Coffin, M., Bradney, A., Baumberger, T., and Wilkinson, C. (2017). "Hydrothermal venting on the flanks of Heard and McDonald islands, southern Indian Ocean," in *Proceedings of the AGU Fall Meeting Abstracts*, Washington, DC.

Maraldi, C., Mongin, M., Coleman, R., and Testut, L. (2009). The influence of lateral mixing on a phytoplankton bloom: distribution in the Kerguelen Plateau region. *Deep Res. Part I Oceanogr. Res. Pap.* 56, 963–973. doi: 10.1016/j.dsr.2008.12.018

Markussen, T. N., Elberling, B., Winter, C., and Andersen, T. J. (2016). Flocculated meltwater particles control Arctic land-sea fluxes of labile iron. *Sci. Rep.* 6:24033. doi: 10.1038/srep24033

Martin, J., and Meybeck, M. (1979). Sampling procedures an outline of sampling procedures is given in Table I. Whenever possible. *Mar. Chem.* 7, 173–206.

McDougall, T. J., and Barker, P. M. (2011). *Getting started with TEOS-10 and the Gibbs Seawater (GSW) Oceanographic Toolbox*. Available at: http://www.teos-10.org/pubs/Getting_Started.pdf (accessed July 14, 2017).

Michaud, A. B., Skidmore, M. L., Mitchell, A. C., Vick-Majors, T. J., Barbante, C., Turetta, C., et al. (2016). Solute sources and geochemical processes in Subglacial Lake Whillans, West Antarctica. *Geology* 44, 347–350. doi: 10.1130/G37639.1

Mongin, M., Molina, E., and Trull, T. (2008). Seasonality and scale of the Kerguelen plateau phytoplankton bloom: a remote sensing and modeling analysis of the influence of natural iron fertilization in the Southern Ocean. *Deep Sea Res. Part II Top. Stud. Oceanogr.* 55, 880–892. doi: 10.1016/j.dsr2.2007.12.039

Mottl, M. J., and McConachy, T. F. (1990). Chemical processes in buoyant hydrothermal plumes on the East Pacific Rise near 21°N. *Geochim. Cosmochim. Acta* 54, 1911–1927. doi: 10.1016/0016-7037(90)90261-I

Ohnemus, D. C., Auro, M. E., Sherrell, R. M., Lagerstrom, M., Morton, P. L., Twining, B. S., et al. (2014). Laboratory intercomparison of marine particulate digestions including Piranha: a novel chemical method for dissolution of polyethersulfone filters. *Limnol. Oceanogr.* 12, 530–547. doi: 10.4319/lom.2014.12.530

Pakhomov, E., and Froneman, P. (1999). The Prince Edward Islands pelagic ecosystem, south Indian Ocean: a review of achievements, 1976–1990. *J. Mar. Syst* 18, 355–367. doi: 10.1016/S0924-7963(97)00112-7

Park, Y.-H., Roquet, F., Durand, I., and Fuda, J.-L. (2008). Large-scale circulation over and around the Northern Kerguelen Plateau. *Deep Sea Res. Part II Top. Stud. Oceanogr.* 55, 566–581. doi: 10.1016/j.dsr2.2007.12.030

Passaro, S., Tamburrino, S., Vallefuoco, M., Tassi, F., Vaselli, O., Giannini, L., et al. (2016). Seafloor doming driven by degassing processes unveils sprouting volcanism in coastal areas. *Sci. Rep.* 6:22448. doi: 10.1038/srep22448

Planquette, H., Sanders, R. R., Statham, P. J., Morris, P. J., and Fones, G. R. (2011). Fluxes of particulate iron from the upper ocean around the Crozet Islands: a naturally iron-fertilized environment in the Southern Ocean. *Glob. Biogeochem. Cycles* 25: GB2011. doi: 10.1029/2010GB003789

Poulton, S. W., and Raiswell, R. (2005). Chemical and physical characteristics of iron oxides in riverine and glacial meltwater sediments. *Chem. Geol.* 218, 203–221. doi: 10.1016/j.chemgeo.2005.01.007

Queroue, F., Sarthou, G., Planquette, H. F., Bucciarelli, E., Chever, F., van der Merwe, P., et al. (2015). High variability in dissolved iron concentrations in the vicinity of the Kerguelen Islands (Southern Ocean). *Biogeosciences* 12, 3869–3883. doi: 10.5194/bg-12-3869-2015

Quilty, P. G., and Wheller, G. (2000). Heard Island and the McDonald Islands: a window into the Kerguelen Plateau. *Pap. Proc. R. Soc. Tasmania* 133, 1–12. doi: 10.26749/rstpp.133.2.1

Raiswell, R. (2011). Iceberg-hosted nanoparticulate Fe in the Southern Ocean: mineralogy, origin, dissolution kinetics and source of bioavailable Fe. *Deep Sea Res. Part II Top. Stud. Oceanogr.* 58, 1364–1375. doi: 10.1016/j.dsr2.2010.11.011

Raiswell, R., Benning, L. G., Tranter, M., and Tulaczyk, S. (2008). Bioavailable iron in the Southern Ocean: the significance of the iceberg conveyor belt. *Geochem. Trans.* 9:7. doi: 10.1186/1467-4866-9-7

Raiswell, R., Hawkings, J., Elsenousy, A., Death, R., Tranter, M., and Wadham, J. (2018). Iron in glacial systems: speciation, reactivity, freezing behavior, and alteration during transport. *Front. Earth Sci.* 6:222. doi: 10.3389/feart.2018.00222

Raiswell, R., Tranter, M., Benning, L. G., Siegert, M., De'ath, R., Huybrechts, P., et al. (2006). Contributions from glacially derived sediment to the global iron (oxyhydr)oxide cycle: implications for iron delivery to the oceans. *Geochim. Cosmochim. Acta* 70, 2765–2780. doi: 10.1016/j.gca.2005.12.027

Raiswell, R., Vu, H. P., Brinza, L., and Benning, L. G. (2010). The determination of labile Fe in ferrihydrite by ascorbic acid extraction: methodology, dissolution kinetics and loss of solubility with age and de-watering. *Chem. Geol.* 278, 70–79. doi: 10.1016/j.chemgeo.2010.09.002

Rauschenberg, S., and Twining, B. S. (2015). Evaluation of approaches to estimate biogenic particulate trace metals in the ocean. *Mar. Chem.* 171, 67–77. doi: 10.1016/j.marchem.2015.01.004

Rees, C., Pender, L., Sherrin, K., Schwanger, C., Hughes, P., Tibben, S., et al. (2019). Methods for reproducible shipboard SFA nutrient measurement using RMNS and automated data processing. *Limnol. Oceanogr. Methods* 17, 25–41. doi: 10.1002/lom3.10294

Resing, J. A., Sedwick, P. N., German, C. R., Jenkins, W. J., Moffett, J. W., Sohst, B. M., et al. (2015). Basin-scale transport of hydrothermal dissolved metals across the South Pacific Ocean. *Nature* 523, 200–203. doi: 10.1038/nature14577

Römer, M., Torres, M., Kasten, S., Kuhn, G., Graham, A. G. C., Mau, S., et al. (2014). First evidence of widespread active methane seepage in the Southern Ocean, off the sub-Antarctic island of South Georgia. *Earth Planet. Sci. Lett.* 403, 166–177. doi: 10.1016/j.epsl.2014.06.036

Schallenberg, C., Bestley, S., Klocker, A., Trull, T. W., Davies, D. M., Gault-Ringold, M., et al. (2018). Sustained upwelling of subsurface iron supplies seasonally persistent phytoplankton blooms around the southern Kerguelen

plateau, Southern Ocean. *J. Geophys. Res. Oceans* 123, 5986–6003. doi: 10.1029/2018JC013932

Schroth, A. W., Crusius, J., Hoyer, I., and Campbell, R. (2014). Estuarine removal of glacial iron and implications for iron fluxes to the ocean. *Geophys. Res. Lett.* 3951–3958. doi: 10.1002/2014GL060199.Received

Sherrell, R. M., Annett, A. L., Fitzsimmons, J. N., Roccanova, V. J., and Meredith, M. P. (2018). A "shallow bathtub ring" of local sedimentary iron input maintains the Palmer Deep biological hotspot on the West Antarctic Peninsula shelf. *Philos. Trans. A Math. Phys. Eng. Sci.* 376:20170171. doi: 10.1098/rsta.2017.0171

Spain, E., Johnason, S., Hutton, B., Whittaker, J., Lucieer, V., Watson, S., et al. (2018). "Shallow seafloor gas emissions near Heard and McDonald Islands on the Kerguelen Plateau, Southern Indian Ocean," in *Proceedings from the GeoHab: Marine Geological and Biological Habitat Mapping*, Santa Barbara, CA, 123.

Stephenson, J., Budd, G. M., Manning, J., and Hansbro, P. (2005). Major eruption-induced changes to the McDonald Islands, southern Indian Ocean. *Antarct. Sci.* 17, 259–266. doi: 10.1017/S095410200500266X

Tagliabue, A., Bopp, L., Dutay, J. C., Bowie, A. R., Chever, F., Jean-Baptiste, P., et al. (2010). Hydrothermal contribution to the oceanic dissolved iron inventory. *Nat. Geosci.* 3, 252–256. doi: 10.1038/ngeo818

Thost, D. E., and Truffer, M. (2008). Glacier Recession on Heard Island, Southern Indian Ocean. *Arct. Antarct. Alp. Res.* 40, 199–214. doi: 10.1657/1523-0430(06-084)%5Bthost%5D2.0.co;2

Thuróczy, C.-E., Alderkamp, A.-C., Laan, P., Gerringa, L. J. A., Mills, M. M., Van Dijken, G. L., et al. (2012). Key role of organic complexation of iron in sustaining phytoplankton blooms in the Pine Island and Amundsen Polynyas (Southern Ocean). *Deep Sea Res. Part II Top. Stud. Oceanogr.* 71–76, 49–60. doi: 10.1016/j.dsr2.2012.03.009

Tonnard, M., Wuttig, K., Holmes, T., van der Merwe, P., Townsend, A., Sarthou, G., et al. (n.d). Dissolved and soluble Fe-binding organic ligands near the Kerguelen Archipelago (B-transect) and in the vicinity of Heard and McDonald Islands (HEOBI voyage – GIpr05).

Trull, T., Davies, D., and Casciotti, K. (2008). Insights into nutrient assimilation and export in naturally iron-fertilized waters of the Southern Ocean from nitrogen, carbon and oxygen isotopes. *Deep Sea Res. Part II Top. Stud. Oceanogr.* 55, 820–840. doi: 10.1016/j.dsr2.2007.12.035

van der Merwe, P., Bowie, A. R., Quéroué, F., Armand, L., Blain, S., Chever, F., et al. (2015). Sourcing the iron in the naturally fertilised bloom around the Kerguelen Plateau: particulate trace metal dynamics. *Biogeosciences* 12, 739–755. doi: 10.5194/bg-12-739-2015

van der Merwe, P., Lannuzel, D., Mancuso Nichols, C., Meiners, K. M., Heil, P., Norman, L., et al. (2009). Biogeochemical observations during the winter-spring transition in East Antarctic sea ice: evidence of iron and exopolysaccharide controls. *Mar. Chem.* 115, 163–175. doi: 10.1016/j.marchem.2009.08.001

Watson, S., Coffin, M., Whittaker, J., Lucieer, V., Fox, J., Carey, R., et al. (2016). "Submarine geology and geomorphology of active Sub-Antarctic volcanoes: heard and McDonald Islands," in *Proceedings of the American Geophysical Union Fall Meeting Abstracts*, Washington, DC.

Wojtasiewicz, B., Trull, T. W., Clementson, L., Davies, D. M., Patten, N. L., Schallenberg, C., et al. (n.d). Unexpected lack of phytoplankton biomass in naturally iron fertilized waters near Heard and McDonald islands in the Southern Ocean. *Front. Mar. Sci*.

Wuttig, K., Townsend, A. T., van der Merwe, P., Gault-ringold, M., Holmes, T., Schallenberg, C., et al. (2019). Critical evaluation of a sea FAST system for the analysis of trace metals in marine samples. *Talanta* 197, 653–668. doi: 10.1016/j.talanta.2019.01.047

Zhang, R., John, S. G., Zhang, J., Ren, J., Wu, Y., Zhu, Z., et al. (2015). Transport and reaction of iron and iron stable isotopes in glacial meltwaters on Svalbard near Kongsfjorden: From rivers to estuary to ocean. *Earth Planet. Sci. Lett.* 424, 201–211. doi: 10.1016/j.epsl.2015.05.031

Conflict of Interest Statement: The authors declare that the research was conducted in the absence of any commercial or financial relationships that could be construed as a potential conflict of interest.